coasts

Article

Regional Patterns of Coastal Erosion and Sedimentation Derived from Spatial Autocorrelation Analysis: Pacific and Colombian Caribbean

Oswaldo Coca and Constanza Ricaurte-Villota *

Marine and Coastal Geosciences Program, Marine and Coastal Research Institute "José Benito Vives de Andréis" (INVEMAR), Calle 25 #2-55, Salguero Beach, Rodadero, Santa Marta 470001, Colombia; oswaldo.coca@comunidad.unam.mx
* Correspondence: constanza.ricaurte@invemar.org.co

Abstract: Coastal erosion is a common phenomenon along the world's coasts. Studying it is complex because such studies must cover large portions of land, and it is necessary to understand the multiple processes that interact in each area, so it is important to recognize regional patterns that allow for defining representativeness in relation to the surrounding dynamics. Spatial statistics can be used in coastal geomorphology to identify and quantify trends in coastal morphodynamics. This study analyzes and interprets the spatio-temporal patterns present in the changes in a shoreline, that is, the processes of erosion and coastal sedimentation in the Pacific and the Colombian Caribbean. The results are derived from the detection of significant changes in the coastline via satellite images. For this study, the shoreline of Colombia was digitized for the years 1986 and 2016, thus obtaining changes in the shoreline at a medium temporal scale. The Global Moran's Index, Local Moran's Index and Getis–Ord Index were used to explain the spatial statistics. The Global I Moran values for the Pacific were I = 0.190, z = 31.063 and p = 0.01, and for the Caribbean I = 0.624, z = 74.545 and p = 0.01, which suggests good grouping in the Caribbean and very low grouping for the Pacific. The local indices (Moran's and Getis–Ord) allowed us to visualize and spatialize the significant points of coastal erosion and sedimentation. According to the results, three conceptual models are herein proposed that relate the indices with the geomorphological characteristics: (a) the greater the geomorphological heterogeneity, the greater the grouping; (b) the greater the geomorphological homogeneity, the lower the degree of clustering; (c) the greater the geomorphological complexity, the lower the degree of clustering. Finally, it is confirmed that coastal erosion and sedimentation processes predominate along low coasts.

Keywords: DSAS; Moran's Index; GIS; coastal geomorphology

Citation: Coca, O.; Ricaurte-Villota, C. Regional Patterns of Coastal Erosion and Sedimentation Derived from Spatial Autocorrelation Analysis: Pacific and Colombian Caribbean. *Coasts* **2022**, *2*, 125–151. https://doi.org/10.3390/coasts2030008

Academic Editor: Enzo Pranzini

Received: 11 May 2022
Accepted: 7 July 2022
Published: 12 July 2022

1. Introduction

Regional patterns show how representative observation locations can be of the dynamics surrounding them. Regarding this, Bracs et al. [1] proposed the concept of "regionally representative" coastal monitoring sites, obtaining a great intensity of measurements by which the patterns and trends observed at these sites in the long term can be representative of other beaches.

The coasts of Colombia, together totaling more than 6000 km, can offer good examples of these spatial differences, since they interact with two seas, the Pacific Ocean and the Caribbean Sea. The two coasts present complexities, which are related to the type of coastal zone (sandy, muddy and rocky) and the marked climatic and oceanographic differences [2], as well as the presence of different marine–coastal ecosystems and socio-cultural diversity [3]. Therefore, it is necessary to develop methodologies to represent such diversity and differences on coasts, which can facilitate decision making and adequate planning in relation to the country's coastal areas.

Coastal erosion or sedimentation processes also cause damages and losses for society and human activities; in turn, this modifies the coastline and coastal geomorphology [4], and so coastal erosion is currently considered a major problem for states [5]. However, it should also be mentioned that coastal erosion or sedimentation is also a natural process necessary to many ecosystem functions. The causes of this phenomenon are diverse and are related to geomorphological, climatic, oceanographic, anthropic, and geological factors [2].

In Colombia, different studies on coastal erosion have been undertaken, starting with the descriptive analyses carried out by Posada and Henao Pineda [6] and Posada et al. [7,8], which generated the first coastal erosion maps of the country from observations of coastal geomorphological features. These studies were later complemented with quantitative analyses through the calculation of changes in coastlines and the use of GIS tools [9–11]. Likewise, semi-quantitative information has been generated with relevance to risk management by conceptually adapting the CVI (Coastal Vulnerability Index) methodology of the USGS [3], which facilitated the generation of maps of the hazard and vulnerability caused by coastal erosion in Colombia [2]. Finally, as part of the Third National Communication on Climate Change, a vulnerability and risk analysis related to climate change was carried out for Colombia, which included shoreline changes and their future projection in relation to SLR (Sea Level Rise) [12].

The aim of this article is to employ spatial autocorrelation statistics to identify and interpret statistically significant changes in the shorelines (erosion and coastal sedimentation), and the results obtained from the DSAS (Digital Shoreline Analysis System), on the two coasts of Colombia (Pacific and Caribbean). Thus, satellite imagery and shoreline detection have been widely developed and used for a long time, and range from the manual digitization of the coastline to proven automated processes [13–16]. In the same way, the quantitative evaluation of changes that occur on coasts using tools such as DSAS [17–19] has been very popular, and there are countless publications on this [9,11,18,20,21]. The use of this metric requires multiple corrections and rules [22] in order to obtain values close to reality, but before defining which method and tools to use, the objective must be defined; that is, one must define the purpose of this metric, and from that, choose appropriate elements.

The concept of spatial autocorrelation [23] is defined as the concentration or dispersion of the values of a variable in space; in other words, it reflects the degree to which objects or activities within a geographic unit are similar to other objects or activities within nearby geographic units [24]. This starts from the first law of geography, or the principle of spatial autocorrelation, proposed by Tobler [25], which states that everything is related to everything else, but close things are more related than distant things.

Spatial statistical analyses, such as the Moran Index, have been used to evaluate the distribution of physical phenomena such as soil erosion [26], rainfall [27], and ecological features [28], generating clustered results similar to those of this study. On the other hand, this process has mostly been applied in human and social studies, in order to evaluate distribution, segregation, and transformations, among other social phenomena [29,30], while other studies have focused on distribution phenomena or spatial autocorrelation theory [31–33].

The objectives of this study are as follows: (1) to find a new reliable method to assess coastal erosion at a regional scale to support the decision-making processes; (2) to identify and analyze the spatial clustering patterns of coastal erosion and sedimentation in the Colombian Pacific and Caribbean; and (3) to examine whether the geomorphological characteristics of the coast are associated with the spatial clustering patterns of erosion and sedimentation. The processes of erosion and coastal sedimentation (changes in the coastline) may show regional trends, as implied by the spatial autocorrelation analysis.

2. Study Area

Colombia is located in the extreme northwest of South America, bordering Central America, and has territory on two coasts, the Pacific Ocean and the Caribbean Sea (Figure 1).

The total length of the two coasts of the country is 6962 km, of which 2253 km is on the Caribbean and 4708 km on the Pacific. The tides in the Pacific are macro-tidal, and in the Caribbean they are micro-tidal; the rainfall has a multiannual monthly average of 7609 mm in the Pacific, while in the Caribbean it barely reaches 400 mm [2].

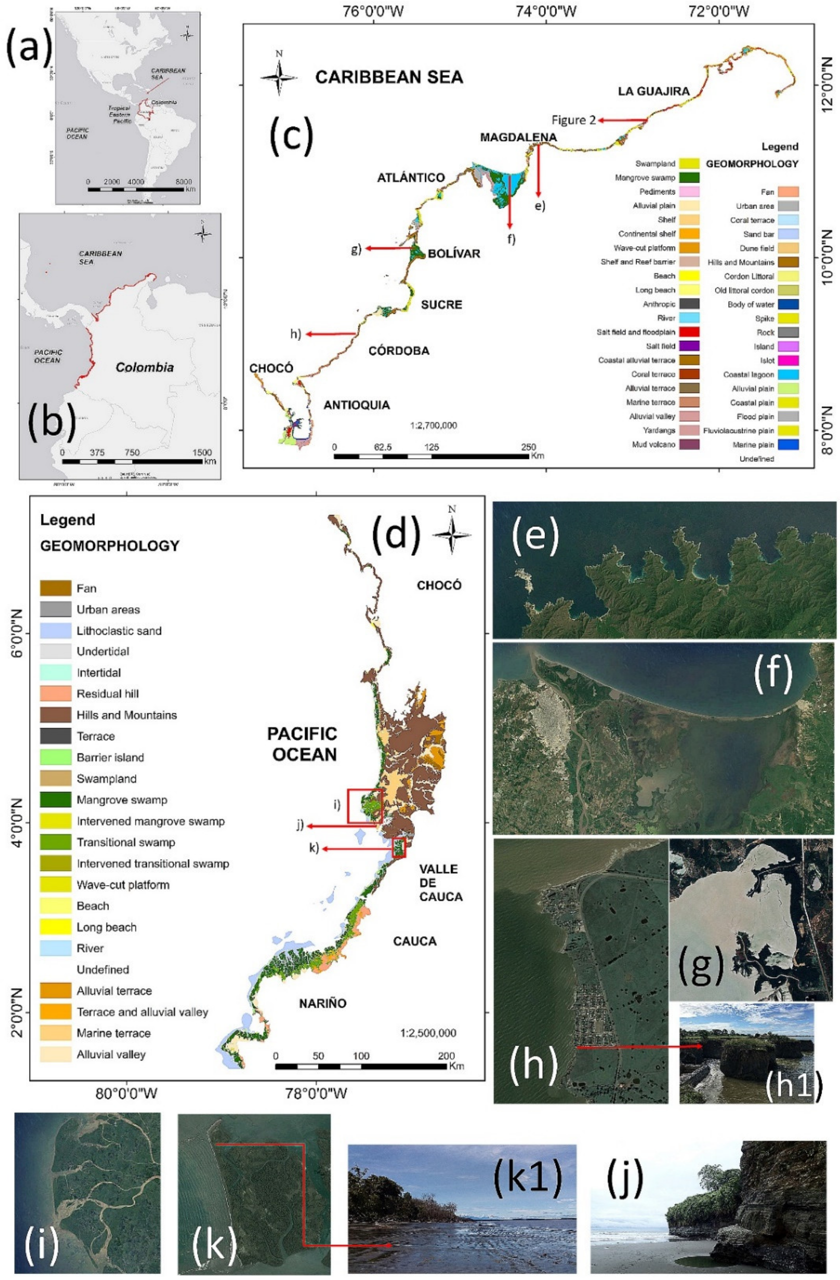

Figure 1. Study area. (**a**) Location of Colombia in northern South America between the eastern tropical Pacific and the Caribbean Sea. (**b**) Location of its coastlines in detail. (**c**,**d**) For the coastlines of the Caribbean and Pacific regions, the coastal geomorphology (developed by Posada et al. [6,7] at a scale of 1:100,000) is shown, along with the units. The green and yellow colors depict low coasts; red to brown depict high shores. (**c**) Figure 2, corresponds to the location of the city of Riohacha, see Figure 2. Examples of some geomorphological units: in the Caribbean: (**e**) Cliffs of the Sierra Nevada de Santa Marta; (**f**) Ciénaga Grande de Santa Marta estuarine complex and mouth of the Magdalena River; (**g**) Deltas of the Canal del Dique; (**h**) Fluvio-marine terraces (**h1**—photo of the place). In the Pacific: (**i**) San Juan River Delta; (**j**) Cliffs in the Ladrilleros sector; (**k**) Isla Barrera El Soldado (**k1**—photo of the place).

The coastal geomorphology of the Pacific presents steep coasts with cohesive rocks, located mostly to the north of Cape Corrientes, while the low coast occupies 76% of the entire coastline and is represented by deltas, barrier islands, muddy coasts, mouths, and beaches, located from Cape Corrientes to the border with Ecuador. For its part, the Caribbean region is characterized by cliffs on its coasts formed from metamorphic–cohesive rocks (Sierra Nevada de Santa Marta), igneous rocks (in Chocó), and sedimentary rocks of calcareous and terrigenous origin; there are also deposits of recent alluvial, colluvial, wind, fluvio-marine, lake, and marine. Along the low coasts, there are deltaic systems (Sinú, Atrato, and Magdalena rivers, and others of smaller sizes), muddy coasts (Cispatá bay) and beaches (La Guajira, Salamanca bar, beaches of San Bernardo del Viento, etc.) [2].

3. Materials and Methods

3.1. Shoreline Change Analysis

Two coastlines corresponding to the years 1986 and 2016 were digitized; for 1986, images from the LandSat 4–5 sensors were used, and for 2016 LandSat 8 images were used, in order to maintain uniformity in the sensor, resolution (spatial and temporal), and scale. The georeferencing of the images was adjusted using images previously georeferenced. These images have been widely used for this type of study, and are suitable for regional and global analysis [14,15].

The process for the selection of the dates of the images had two factors: the temporality—that is, the oldest (1986) and the most recent (2016) available for all of Colombia were taken—and second, the unification of criteria; we use the same sensor at the same spatial resolution, that is, images with different pixel sizes were not used. (In this case it was the LandSat). The use of two images 30 years apart allows us to determine the trend in the evolution and eliminate climatic variability (seasonal, interannual, and decennial), verified by Crowell et al. [34] and Douglas and Crowell [35], as well as the short-term anthropic effects that are generated along the unconsolidated coasts. Analyzing the seasonal or temporary effects is not the objective of this study.

Photography errors were controlled in the georeferenced images, which was carried out by comparing the registered images with the most recent image (2016 image), and by means of the root mean square error (RMS), calculated using GCPs as reference points for each image, which gave us a geometric precision of approximately <3.0 m [22,36].

All the images were orthorectified assuming a flat terrain, which enables minimum distortion of the image at sea level [22], and were set in the same coordinate system [36]. The Ground Control Points (GCPs) were obtained for the most recent satellite image (2016), and approximately 20 to 30 GCPs were used in each image; their positions varied for each image [37]. In the different stages of this process, the error accumulates, so that within the uncertainties of the shoreline, a combination of the Mean Square Error (RMS) was related to the differences in the location of the GCP, the quality of the image (pixel) and coastline mapping (digitization error) are the method recommended by Radosavljevic [22]. The DSAS also contributes in this stage, since it takes into account the uncertainty for the analysis of the movement of the coastline, providing statistical robustness [19]. The average cumulative total error was 26.65 m.

To digitize the shoreline, the HWL proxy (High Water Line) [38] was used, and also the recommendations of Ojeda Zújar et al. [39] were used. This was carried out using a single digitizer (a thematic expert) to reduce subjectivity, and at a scale of 1:2500 for geometric coherence. The criteria had an ecological basis, defined by geomorphological and physiographic characteristics [39]. The standardization of the tidal error and the storm wave begins with the digitization of the coastline for the calculation of coastal erosion [39], which combines long and short coastlines. This criterion allows for the elimination of tidal errors in the Pacific (meso- to macro-tidal) and Caribbean (micro-tidal) regions (Figure 2).

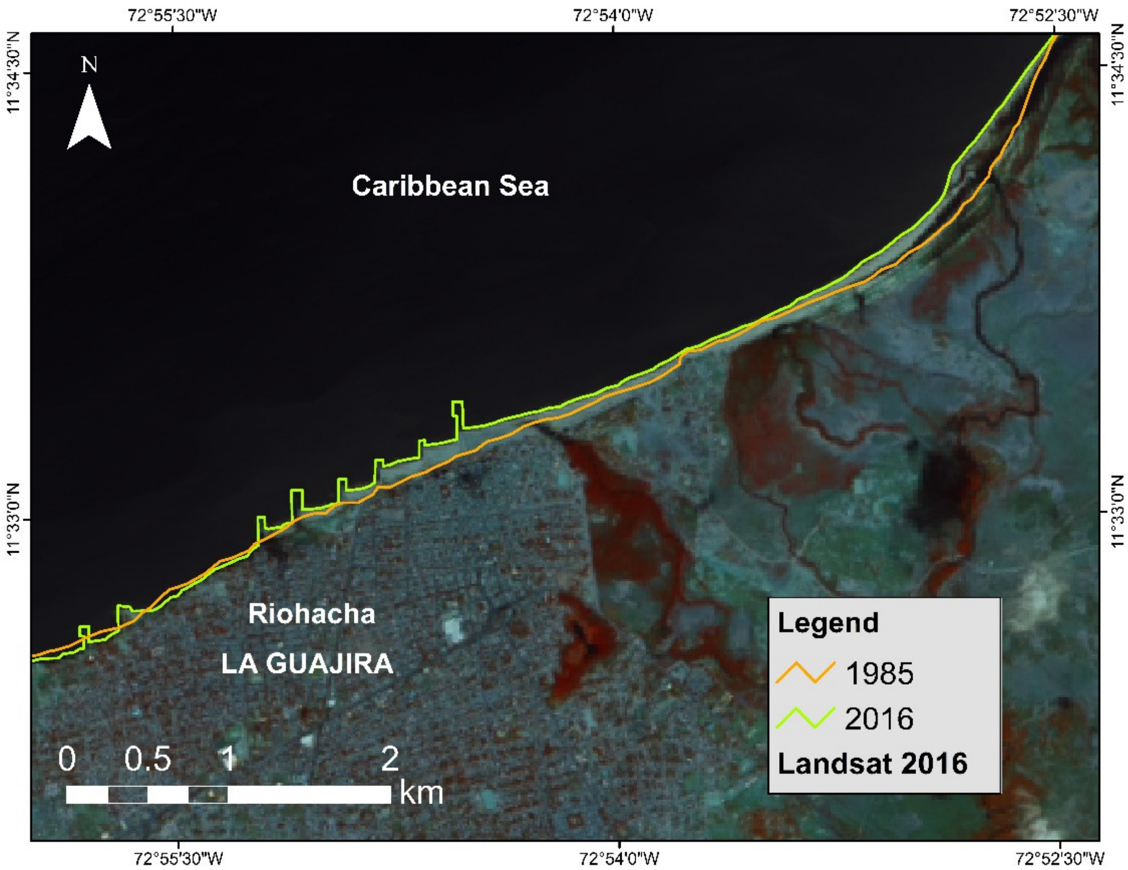

Figure 2. Digitized shorelines, following the parameters of Ojeda Zújar et al. [39] and the HWL as a proxy. The coastlines correspond to the years 1985 and 2016 in the city of Riohacha (La Guajira), for location, see Figure 1c.

The analysis was carried out with the DSAS (Digital Shoreline Analysis System) extension, a tool that calculates the statistical parameters of coastlines changes for specific periods. This analysis was carried out at the departmental level (political division of Colombia). The extension requires transects perpendicular to the coastlines that are drawn automatically and were each 200 m apart; at the regional and global scales, the transects were generated every 250 m [15], or every 500 m [14]. The use of the DSAS yielded data on the displacement of the coastline in attribute tables, and facilitated the calculating of statistical parameters indicating status and changes in the specific periods already determined in this study. Within this work, the following statistical parameter was used:

- End Point Rate (EPR). This is defined as the ratio of the distance between the oldest and the most recent coastline, over the period (in years) between both lines [17]; it is defined in distance over a unit of time (m/year).

The advantage of the EPR method is that it is simple [22]. The limitations are that only two points are used; therefore, seasonality and its magnitude changes, and cyclical trends in shoreline movement, can be overlooked [19,22,40], but as we have already said, this is not the objective of this study. Radosavljevic et al. [22] compared different statistics with the EPR, and found that the EPR is more conservative than LRR (Linear Regression Rate) and WLR (Weighed Linear Regression) [17].

When using DSAS, the simplicity of the EPR can be convenient for the analysis of spatial autocorrelation via regional patterns (the objective of this study), since negative or positive values are taken from trends in the changes in coastlines, or from only two points. Considering that there are multiple types of coastlines showing temporary (beaches, mangroves, etc.) or permanent (cliffs) coastal erosion, the use of EPR or linear regressions

(LRR or WLR) with seasonal correlations should not be detrimental to the results. Spatial variables and analyses are essential elements when exploring geographic patterns, and this process of visualization relies on computer-based Geographic Information System (GIS) software and technology [41].

Sources of shoreline uncertainty can include pixels, digitization, rectification, and seasonal and tidal fluctuation errors [42]. Pixel error refers to the spatial resolution of an image, and corresponds to the image resolution in digital photographs [22]. The uncertainty of the interpretation of the position of the coast is called the digitization error (in this study, a single operator performed digitization) [22].

In order to be able to use coastal positions obtained from satellites for different analyses, such as estimating trends and changes in coasts, a horizontal resolution of at least 10–20 m is required; for example, a coast with rates of change of 0.5 m/year over three decades would have a tendency towards erosion or sedimentation of 15 m [14]. Here, it should be clarified that long-term trends unfold over decades to centuries [43]. In this context, Luijendijk et al. [14] stated that different authors [21,44–47] have found that the positional precision of coasts when derived from satellites, via individual images, ranges between 1.6 and 10 m. However, Hagenaars et al. [48] analyzed trends in coasts using long-term and local-scale satellite images, and overcame all the aforementioned limitations. Here, the coastal images derived from satellite images constructed out of a moving average showed sub-pixel precision (approximately half pixel size); when applied to Landsat 4–5 images (30 m), this precision would correspond to 15 m. The ~15 m precision of Landsat images reported by Hagenaars et al. [48] coincides with the displacement required for reliable classifications of coastline change over the last 30 years (10 to 20 m). Luijendijk et al. [14] took the same approach as Hagenaars et al. [48] but on the global scale. Our study applied this approach on a regional scale to define uncertainty, but we decided to expand this to identify areas with better-defined long-term trends, thus making it useful for the subsequent analysis of the spatial autocorrelation of coastal erosion and sedimentation.

Finally, for the classification of shoreline rates, we considered that Landsat 4 and 5 images have a spatial resolution of 30 m per pixel, while Landsat 8 (with a Panchromatic sensor) can resolve 15 m. Taking into account the fact that the pixel size was 30 m and the evaluation time was 30 years, to obtain the margin of error in units of change rates (m/year), the resolution distance was divided over the period between images (30 m over 30 years), obtaining an uncertainty range of 1 m/year (that is, between -1 and 1 m/year). Therefore, the EPR values obtained within this range were not taken into account, and were considered within the range of uncertainty or stability, allowing us to eliminate the possible seasonality in low coasts.

For the analysis of the results of the change rates, the statistical median (given by department) was used, which helped in verifying the relation between the behaviors in each zone and in each region.

3.2. Spatial Autocorrelation

The implementation of spatial autocorrelation is not uncommon in coastal geomorphology; however, spatial statistics are generally underused in coastal geomorphology, despite offering great potential for identifying and quantifying spatio-temporal trends in landscape morphodynamics. That said, they have been used for studies of erosion and sediment deposition in beaches and dunes [49,50]. These authors used LIDAR technology to generate Digital Elevation Models (DEM) of a beach, and through the Moran Local Index, they identified erosion and deposition zones. They also adapted Nelson and Boots's [28] conceptual scheme to geomorphological processes; we also adapted this scheme to the processes of changes in coastlines (coastal erosion and sedimentation).

The local Moran I provides a statistical framework for detecting clusters of significant changes in an attribute, and quantifying how this changes over space and time [49]. However, the simple presentation of a set of I and Z Moran values may not help to identify the mechanisms of sedimentation and erosion underway around coasts, but through spatial autocorrelation, we may be able to more effectively infer these mechanisms, and thus more clearly understand the phenomena on two coasts with environmental differences. Eamer and Walker [49] used the local Moran's Index to identify zones of erosion and deposition on a beach, and geomorphic changes from a DEM, relying on the index's geomorphological relevance. The exploratory use of the index allowed them to identify patterns in their study area, one of which is that the intuitive interpretation of the extreme groupings (HH and LL), which they identified as Dh and Ec, corresponds to deposition and erosion processes, respectively. They used a conceptual scheme adapted from Nelson and Boots [28], which we too adapted to this study. In addition, we used the same premise to identify the patterns of erosion and coastal sedimentation: Sh and Ec, respectively. This is all inferred from the metric of changes in the coastline. The results of Eamer and Walker [49] validate our interpretations.

3.2.1. Geospatial Approach

To analyze the spatial distribution of coastal erosion and sedimentation along the coastline, the spatial autocorrelation was calculated [24], which can elucidate the dependence [51] and the spatial heterogeneity [52,53] of the phenomena via the Moran Index, which is estimated using global and local indicators of spatial autocorrelation.

The statistical significance of the z-values (z-score) of coefficient I (Moran's Index) was tested, with the assumption of normal distribution [23,24]. To check the significance of the spatial autocorrelation, the results of the statistical *p*-value were used, which enables us to reject the null hypothesis. Statistical tests, for the most part, begin with identifying a null hypothesis, which involved using pattern analysis tools (cluster assignment) to determine the complete spatial randomness of the entities, or the values associated with those entities. The z-scores and the *p*-values generated by the pattern analysis tools may or may not enable us to reject the null hypothesis. Here, the following statement is taken as the null hypothesis: "*the spatial configuration occurs randomly*". The alternative hypothesis is "*the spatial configuration does not occur randomly*" [30,54].

This approach can also indicate whether, instead of a random pattern, the entities (or the values associated with the entities) are clustered, or have a statistically significant dispersion [55]. In other words, the *p*-value of pattern analysis tools always includes the probability that the spatial pattern has been created by some random process. When the *p*-value is very small, it means that it is very unlikely that the observed spatial pattern is the result of random processes; therefore, one can reject the null hypothesis [30].

On the other hand, the z-scores indicate standard deviations, and the higher or lower the value, the greater the intensity of the grouping. A positive z-score indicates that there is a grouping of high values, which indicates that processes with extreme values are grouped in greater intensity, namely, erosion or coastal accretion. These data, together with the NPL values obtained as a whole and as interpreted, help us to determine whether the result of the analysis is statistically significant according to the level of confidence [32].

Analyses were performed for the two regions (Caribbean and Pacific) separately. Negative and positive values (above the uncertainty level) were obtained from the changes in the shoreline, that is, the EPR results extracted from the DSAS. After this, the spatial weights and neighborhood matrix were generated, and were incorporated as a file (.swm) into the processing of the global and local Moran's Index, all of which was executed in ArcGIS. The values can be seen in Table 1.

Table 1. Generated spatial weights matrix. The default neighborhood search threshold was 4323.4261 m for the Caribbean and 2712.9342 m for the Pacific.

Region	Number of Feature	Percentage of Spatial Connectivity	Average Number of Neighbors	Minimum Number of Neighbors	Maximum Number of Neighbors
Pacific	7755	0.43	33.04	1	84
Caribbean	4111	0.85	35.09	1	79

As mentioned before, the two spatial analysis techniques commonly used to evaluate spatial clustering patterns are global and local. First, global grouping, using the global Moran's Index, has been populated and supported in previous studies [30,41,56], and measures general patterns in a specific area without delineating exact locations, while the local grouping evaluate patterns at a small scale in the study area [41,57]. This allows the results of the local analysis to be mapped, showing the locations of the identified clusters. Here, we used a local cluster detection measure, Anselin's Local Moran's I (LISA) [58], and hot spots [59–61]. Both levels of grouping have different meanings and possible interpretations, and can be used in complementary ways [41].

The manual computation of this process is laborious; therefore, these analyses were facilitated in a GIS environment, and were complemented using ArcGIS and GeoDa software [62].

3.2.2. Global Moran's Index

The Moran Index [63,64] measures the tendency of similar values to group together in space, and is scored between 1 and −1, where 1 is positive autocorrelation, −1 is negative and 0 implies the non-existence of a defined pattern. This statistic can be calculated from the equation proposed and reviewed by Cliff and Ord (1969) and Goodchild (1986) [23,24].

To execute this analysis, ArcGIS 10.6 was used through the Spatial Autocorrelation (Moran's I) tool, which, in the global spatial measurement of Moran I, implements the statistic as follows:

$$I = \frac{n}{s_0} \frac{\sum_{i=1}^{n} \sum_{j=1}^{n} w_i, j^z i^z j}{\sum_{i=1}^{n} z_i^2}, \tag{1}$$

where I = the I statistic of Global Moran for the spatial, n = sample size, i = individual observation, j = observations at other locations, w_i, j = the spatial weight matrix (distance threshold, see Table 1), x_i = individual z-score value, and S_o = the aggregate of all spatial weights [63,64]. Each feature is analyzed within the context of neighboring features located within the distance that you specify for the threshold distance. Neighbors within the specified distance are weighted equally.

The null hypothesis was that there is no spatial clustering in coastal erosion and sedimentation in the Pacific and Caribbean regions, and our analysis has produced a general clustering estimate for the entire country [64]. Finally, the distribution of the points analyzed in the adapted figure of the Moran scatter plot quadrant (proposed by Nelson and Boots [28] (standardized mean of neighborhood)) was determined using GeoDa software [62].

3.2.3. Local Moran's Index and Local Getis–Ord

The Local Indicators of Spatial Association (LISA) method allows one to expand the spatial autocorrelation analysis by recognizing "local patterns" of spatial identification [30]. This is achieved via a disaggregation of the index (the Moran Local Index or the hot spots), which allows us to check how much each spatial unit contributes to the global behavior of the analyzed phenomenon [54]. The LISA cluster measures the association between the values of one unit and those of neighboring units (in this case, EPR vs. EPR), and this analysis produces analytical results for each individual in the data set [41].

The local Moran Index defines the degree of grouping in the distribution of four types of cluster: High–High (high center, high surrounded), Low–Low (low center, low surrounded), Low–High (low center, high surrounded), and High–Low (center high, surrounded low) [28]. To run this analysis, the ArcGIS tool was used in Cluster and Outlier Analysis (Anselin Local Moran's I).

The LISA statistic for each individual was calculated as follows [58]:

$$I_i = \frac{(x_i - x)}{\sigma^2} \sum_{J=1}^{n} w_{iJ}(x_J - x), \tag{2}$$

where I = local Moran's I statistic for localized spatial autocorrelation, n = sample size, i = individual observation and j = observations in another location, x_i = value of individual z-score, x = mean value of z-score, σ^2 = variance in z-score, and w_{ij} = spatial weighting (distance threshold, see Table 1).

Another analysis that was implemented was the local Getis, which uses other statistics in the same way as the Local Moran Index, and allows one to individually locate the indicative values of the autocorrelation. The local Getis statistic only considers positive spatial autocorrelation (cluster), and allows for differentiation between groups of values that are high or low relative to the mean [28,59]. Using the local Getis statistic, it is possible to identify the spatial groupings of large and small attribute values. After identifying the groupings of large and small values, referred to as hot spots and cold spots (equivalent to the High–High and Low–Low groups, respectively), the Local Moran Index is identified.

The ArcGIS tool Hot Spot Analysis (Getis–Ord G_i*) was used, which uses statistics in the following way:

$$G_i^* = \frac{\Sigma_j w_{ij} X_j}{\Sigma_j X_j}, \tag{3}$$

For G_i*, the value of i is included in the sum, and the attribute relation is defined as $y_{ij} = x_i + x_j$. Here, x_j is the attribute value for feature j, w_{ij} is the spatial weight between features i and j, and n is equal to the total number of features [59,61].

4. Results

In general terms, coastal erosion in Colombia affects 30% of the coastline of the country; that is, approximately 2085 km of coastline is subjected to some coastal erosion process, which is almost equivalent to the Colombian Caribbean coastline. On the other hand, 48% of the country's coastline falls within the range of uncertainty. Finally, 22% of Colombia's coast displays sedimentation, which means a significant contribution is still being made by sediment.

The Colombian Pacific presented erosion along 32% of its coastline, which is 3% more than the Colombian Caribbean coastline (29%). On the Pacific coast, approximately 1412 km is affected, and on the Caribbean side, it is only 675 km; this difference is related to the geomorphological characteristics of each region, whereby the deltas of the rivers in the Pacific are dominated by tides, generating ebb and flow processes, which are tidal currents with great dynamic effects that transport sediments at high speed, thus modifying the coastal zone [65].

4.1. Variation in the Colombian Coastline 1986–2016 (Regional Characteristics of Caribbean and Pacific Coasts)

The analysis of the variation in the Colombian coastline between 1986 and 2016, based on the departmental median (Figure 3), has shown that, on the Caribbean coast, six of the eight departments have negative values (regional variability), indicating a decline in the shoreline. A general characteristic observed in these results (see graphs of transects within Figures 4–6) is that the erosion and sedimentation processes are grouped, or are generally found in long segments of the shoreline, and settle in a geomorphological unit.

In the northern zone of the department of La Guajira, the greatest changes (erosion and sedimentation) were observed within bays and towards the low coasts, near the border with Venezuela (Figure 4). These changes are mainly due to variations in mangrove cover. In the city of Riohacha, sedimentation processes were observed, which were associated with the protective infrastructure built on the beach. Non-cohesive rock cliffs such as marine terraces, abrasion platforms, or hills of sedimentary origin, which have a high degree of erodibility, were present. Sites such as Palomino, Manaure, Puerto Estrella, Ballenas, and Punta de los Remedios have erosion rates greater than 1 m/year.

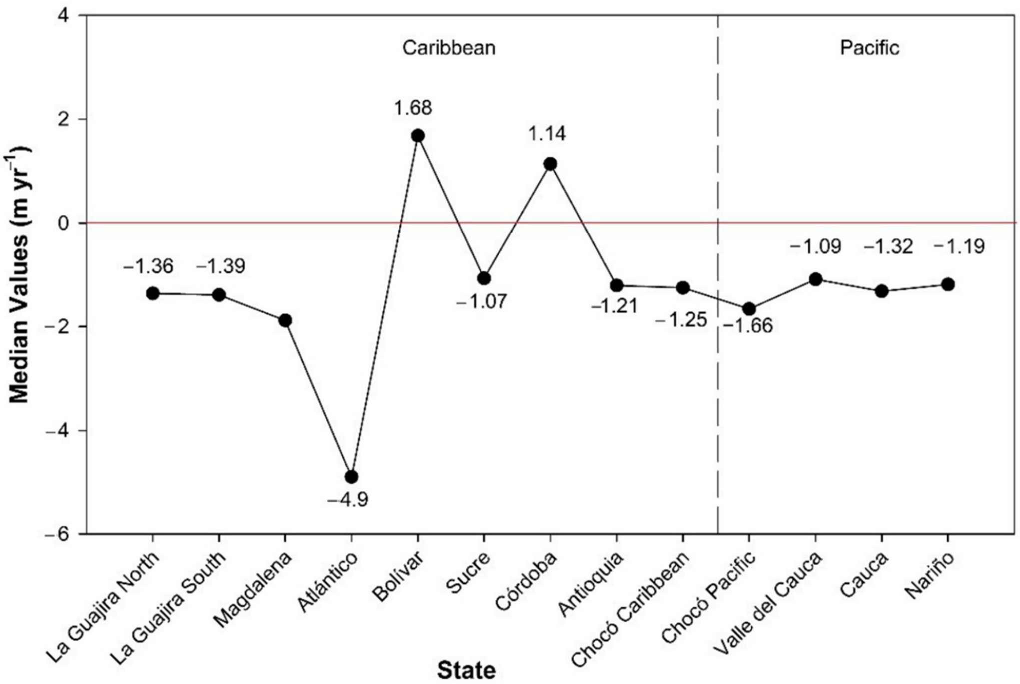

Figure 3. The median change rates (m/year) by department, only using data outside the range of uncertainty. The dashed black line divides the departments of the Caribbean to the left and those of the Pacific to the right. The red line shows the zero value. States are departments.

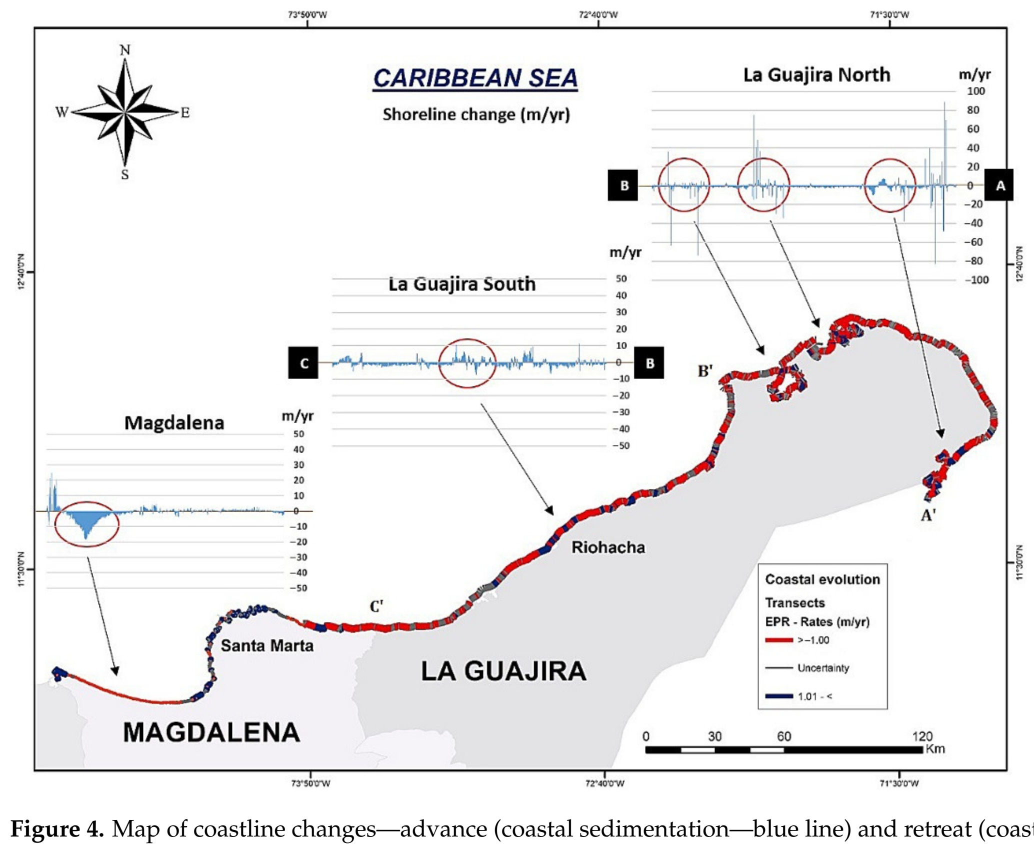

Figure 4. Map of coastline changes—advance (coastal sedimentation—blue line) and retreat (coastal erosion—red line)—for the departments of La Guajira and Magdalena (Colombian Caribbean). The graphs show the DSAS results on the shoreline; the x-axis values correspond to the ID of the transects generated, and the y-axis values correspond to the EPR change rates (m/year). The shoreline of the department of La Guajira was divided into two transects A–B (A′–B′) and B–C (B′–C′).

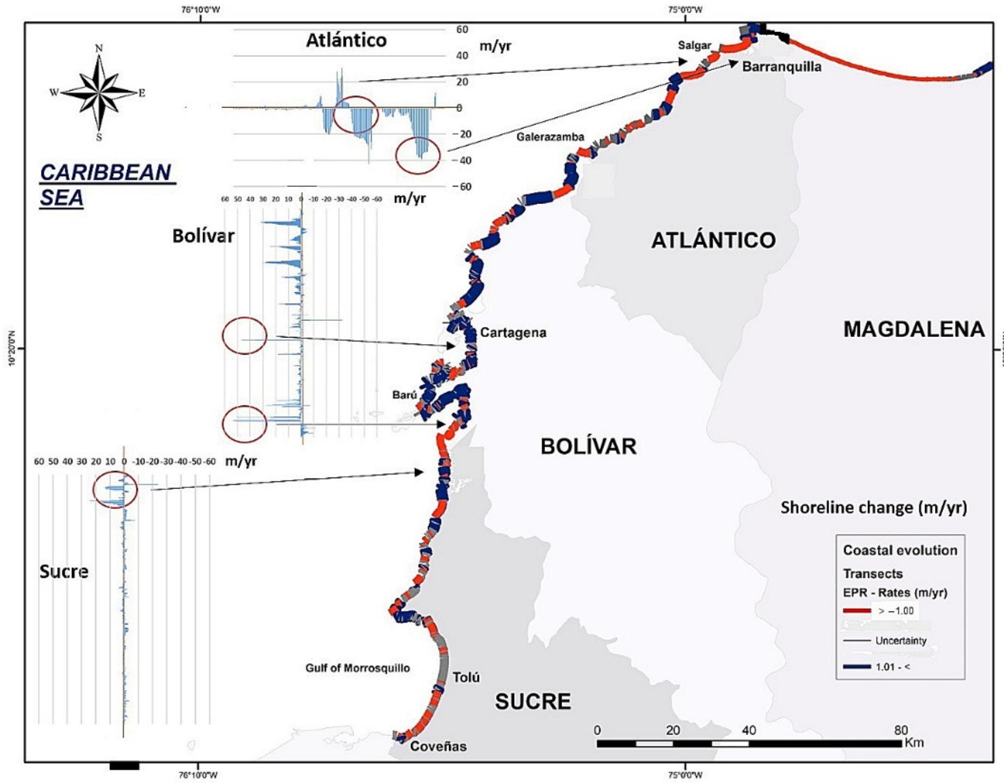

Figure 5. Map of coastline changes—advance (coastal sedimentation—blue line) and retreat (coastal erosion—red line)—for the departments of Atlántico, Bolívar, and Sucre (Colombian Caribbean).

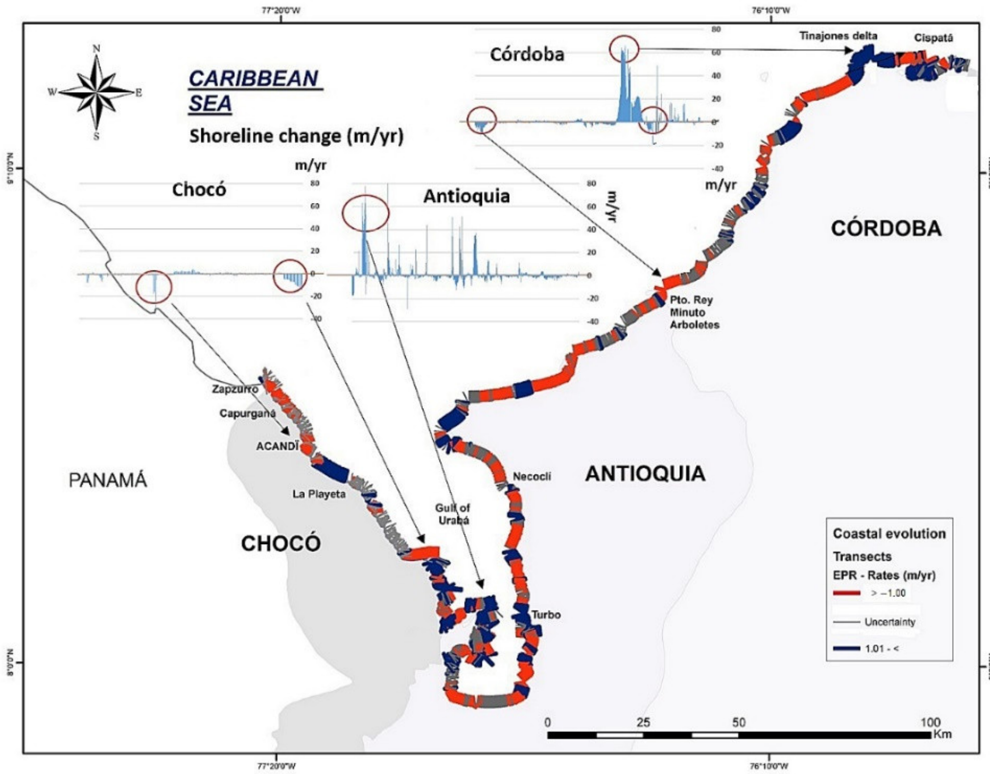

Figure 6. Map of coastline changes—advance (coastal sedimentation—blue line) and retreat (coastal erosion—red line)—for the departments of Córdoba, Antioquia, and Chocó (Colombian Caribbean).

In the departments of Magdalena and the Atlántico, increases are observed in the values of coastal erosion (Figure 3); between these two sectors is located the mouth of the Magdalena river (the most important in the country), which has the highest levels of sediment discharge [66,67]. To the northeast of the mouth (dep. Magdalena), the Salamanca bar is located, as well as the largest coastal lagoon in Colombia (Ciénaga Grande de Santa Marta), comprising mangroves, beaches, dunes, and estuaries, with rates close to −20 m/year. Coastal erosion has been permanent during recent decades, generated by the construction of a highway that blocks the passage of sediment between the swamp and the sea [2], where there is only an opening of approximately 200 m [68]. Stable areas are present in the metamorphic rock cliffs of the Sierra Nevada de Santa Marta; the beaches of this area are situated within bays, and are thus sheltered (Figure 4). Different anthropogenic factors, such as the construction of the Magdalena river jetty and other works related to the port of Barranquilla, have impacted this area (erosion and sedimentation, ecosystem changes) [69], the loss of islands such as Mallorquín (in the Atlantic) or Los Gómez (In Magdalena), and the loss of coastal arrows such as Isla Verde and Sabanilla [70]. On the other hand, from La Guajira to Bolívar, the waves are higher [71]; however, in addition, the extreme waves generated by cold fronts and storms impact this area more frequently [72]. To the southwest of the Magdalena River mouth are geoforms, such as fluvial deposit, beaches, bars, lagoons, and littoral spikes (Figure 5).

The department of Atlántico has the highest negative change rates in the Caribbean and the country. Sectors such as the Ciénaga de Mallorquín, Puerto Colombia, and the Ensenada Rincón Hondo have presented retreat of the coastline with values between −20 and −40 m/year, being those characterized by alluvial deposits (Figure 4); one of the causes of such high retreat values is due to the construction of the navigation channel at breakwaters of Bocas de Ceniza at the Magdalena River, which has diverted the supply of sediments, preventing them from reaching the coasts.

The department of Bolívar, on the contrary, presented positive values in coastline changes (1.68 m/year) with rates between 30 and 50 m/year, in sectors near the mouths of the Canal del Dique, related to the contribution of sediments of the Magdalena River; in the same way, on this area of the Caribbean there is a geological variability, with a presence on the coastal area of calcareous and terrigenous sedimentary rocks, and recent deposits such as beaches, fluvio-marines, marines, and lacustrine. Finally, the negative rates only reached maximum values between −10 and −30 m/year in the south of the department, where low lacustrine coasts are located [67] (Figure 5).

In Sucre, changes occurred in the northern sector, near to Punta Sabanetica, such as erosion processes occurring in exposed areas (normal in these geoforms), but sedimentation could be observed nearer to the sheltered area, while the Gulf of Morrosquillo presented values within the range of uncertainty, generated by the large amount of coastal infrastructure in the area (Figure 5).

In the department of Córdoba, several situations can be observed; the first relates to the mouth of the Sinú River (delta), where positive rates of change are reached indicating sedimentation with values of up to 66.34 m/year. Cispatá Bay shows negative rates of −20 m/year. While the beaches of San Bernardo del Viento have suffered a decrease in the same way, almost the entire southern area is characterized by terraces of terrigenous origin, presenting a definitive decline, with the towns of Minuto de Dios and Puerto Rey being the most affected, in addition to some rocky points with negative values where the highest rates reached −20 m/year due to it receiving the strong waves of the dry season and the north trade winds at the base of the slope. It is also affected in the rainy season by runoff water, which gives rise to furrows and erosion [20] (Figure 6).

In Antioquia, positive values of change can be observed in the delta of the Atrato River, reaching values higher than 60 m/year, while negative changes in the coastline were observed in the Zapata and Damaquiel sectors, with this being the longest sector with coastal erosion and characterized by being the continuation of terraces or sedimentary deposits of terrigenous origin (Figure 6). In the Caribbean part of the department of

Chocó, the sectors of Zapzurro, Capurganá, and Acandí, located to the north and center, respectively, presented negative changes in the coastline, as did the southern part of the department, reaching rates of up to −15 m/year. Only the Playetas sector, a long beach that reaches 14 km in length, presented positive changes. These variations were only observed in the low coasts, since in the coastal region of this department, there are rocks and cliffs of volcanic origin that generate stability (Figure 6).

In the Colombian Pacific (Figure 3), the trend was negative in all departments. A homogeneous trend was observed in the Pacific with respect to the Caribbean, which shows greater variability by department.

In general, there is great variability between the sedimentation and erosion processes in short segments of the shoreline (see transect graphs in Figure 7). The most important characteristic is that, from Cabo Corrientes to the north, high coasts predominate, and from Cabo Corrientes to the south, low coasts predominate (Figure 7a) [2,65,73,74]. Towards the north, erosion values are observed in the beaches and mangrove areas within the bays, and these are grouped almost without exception. It should be remembered that despite the geological and geomorphological differences between the northern and southern sectors of the Pacific region, there are also differences in the climatic and oceanographic processes [2].

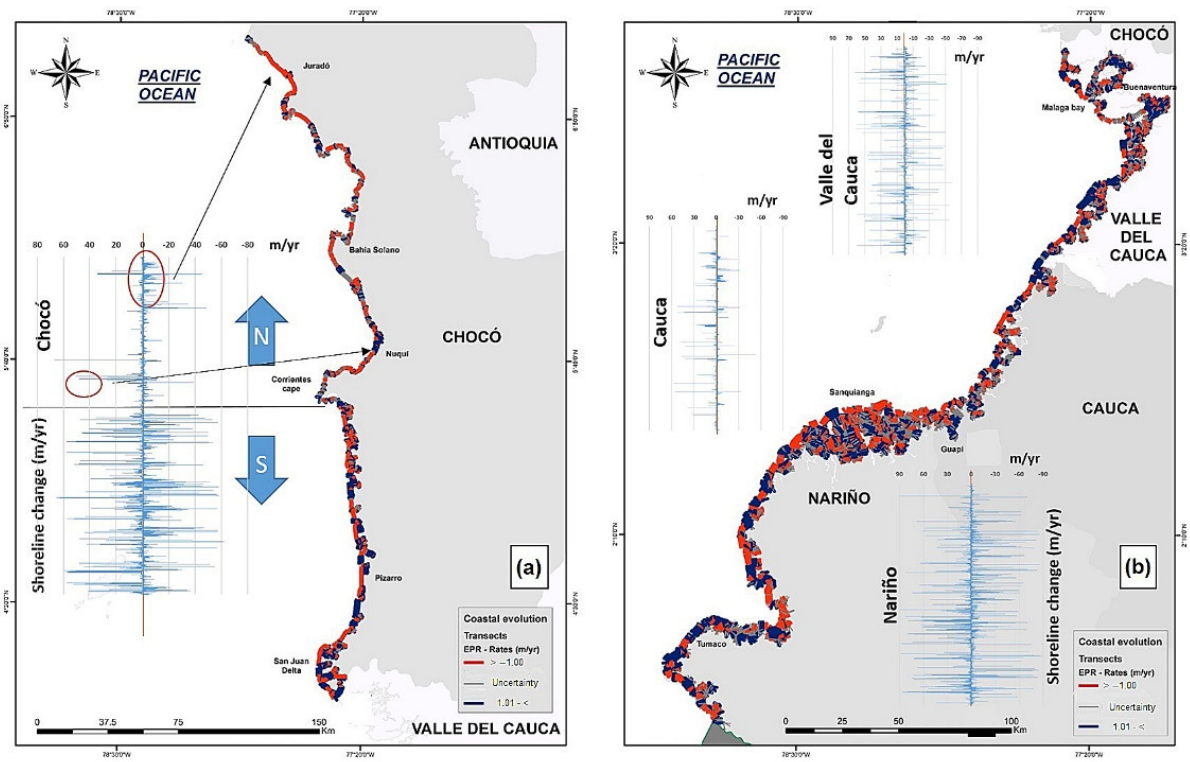

Figure 7. Map of coastline changes—advance (coastal sedimentation—blue line) and retreat (coastal erosion—red line)—for the department of Chocó (**a**) and the departments of Valle del Cauca, Cauca and Nariño (**b**) (Colombian Pacific).

The department of Chocó presented values of −60 and 40 m/year in the southern zone, where low and depositional coasts predominate, with high dynamics of the mouths of rivers and estuaries that maintain a very high variability of change. On the other hand, in the north, there are no negative changes in the beaches and only in the cliffs, and there are rates in the range of uncertainty or stability; it can be observed in a general way in the department that there is a great variability between the processes of accretion and erosion (Figure 7a).

The Valle del Cauca also presented variability in positive and negative values over its entire coastline, dominated by barrier islands, mangroves, beaches, cliffs, channel mouths, river mouths, and bays. On the steep coasts located to the north, stability values were observed; only inside the bays (Málaga and Buenaventura) were accretion processes present (Figure 7a).

In the department of Cauca, variability can also be observed, but this time associated with the low coasts; in this area there is only presence of this type of coastline, related to beaches and mangrove swamps. The negative values of the change rates of greater magnitude were observed to the north of the department, and the rest was interspersed between negative and positive values (Figure 7b).

Finally, in the department of Nariño, as in Valle del Cauca, Cauca, and Chocó, there are negative and positive values interspersed, showing the variability in the Pacific coast of Colombia, which makes it dynamic and with change values between 40 and 70 m/year. On the Nariño coast is the deltaic system of the Sanquianga National Natural Park, followed by some small stretches of rocky coasts, but mostly low sandy coasts and mangrove swamps, until reaching the delta south from the Mira River near the border with Ecuador (Figure 7b).

In the southern zone (Figure 7b), where low and depositional coasts predominate, with dynamic river mouths and estuaries, the meso- to macro-tidal system and the climatic conditions (including high rainfall) [2] maintain a trend of great variability, represented by the sedimentation and erosion processes observed in very short stretches of shoreline (see the transect graphs). This area is dominated by low coasts, characterized by the presence of barrier islands, mangrove areas, bars, beaches, river mouths, river and bay mouths, estuaries, and ebb and flow tidal currents. Castelle et al. [75] show the change in the coastline with the presence of two large-scale tidal inlets, the mouth of an estuary, and some coastal cities, and their results suggest a great spatial and temporal variability. They propose that the coasts adjacent to the inlets and the mouth of the estuary are the most dynamic, alternating erosion and accumulation over time (decades). Other studies of changes in the shoreline carried out on estuarine coasts show similar behaviors [76–78].

The deltaic systems of the Pacific (Rios San Juan, Sanquianga, and Mira) behave differently from those of the Caribbean (Magdalena, Sinú, and Atrato rivers) [67,79]. In the Pacific, the variability between erosion and sedimentation is maintained in short stretches of shoreline, while in the Caribbean, erosion and sedimentation are observed in each delta. Despite this grouping or accumulation of erosion and sedimentation processes in long segments of the coast, they were also observed in other geomorphological units of the Caribbean. Mentachi et al. [15] suggest that the installation of dams, irrigation systems, and structures that modify the flow of sediments is one of the factors that promote changes in the shoreline, among others. The results show that the size of the observed changes (grouped), can differ greatly between the coastal stretches, which can range from more than 1 km to tens of kilometers, showing, for example, the Indus delta, some parts of the Bohai, or the Kazakh Caspian coasts.

4.2. Spatial Autocorrelation of the Rates of Change in the Coastline

4.2.1. Global Moran's Index

The spatial autocorrelation on the Caribbean coast is significant (0.624), while that on the Pacific side is very low (0.190); according to the classification of Siabato and Guzmán-Manrique [32], these values indicate that the two regions present a positive spatial autocorrelation with a cluster pattern. That is to say that similar values are grouped on the same map, and a grouping phenomenon predominates (Table 2).

Table 2. Results of the Global Moran Index and average nearest neighbor.

Region	Global Moran's I		Local Moran's I	
	Index Value	**z-Score**	**High-High Cluster Observations [1] (#,*,%)**	**Low-Low Cluster Observations [1] (#,*,%)**
Caribbean	0.587	25.33	313, 6	350, 6.7
Pacific	0.275	8.61	402, 5.1	366, 4.7

[1] *p*-value: * $p < 0.05$; # *(number of observations)*; % *(percentage of observations)*.

The z-score is used to test this hypothesis; for the Caribbean, the score was 74.545, which represents a probability of less than 1% that the grouping pattern could be the result of a random cause. Similarly, the Pacific obtained a z-score of 31.063 (Table 2). According to these data, the null hypothesis is rejected, and an alternative hypothesis (with statistical significance of 95%) is accepted, stating that there is a high degree of spatial aggregation, specifically between high values (whether negative or positive), that is, sedimentation processes and coastal erosion.

4.2.2. Local Getas–Ord

The Getis–Ord results show that larger neighborhood sizes result in more centroids with significant spatial patterns (Table 3). Visually, hot regions show consistency in terms of location (Figure 8). The local grouping results can be seen in Table 3. The Colombian Pacific showed 14.58% cold spots and 99% hot, while in the Caribbean, 20.28% of the entire sample was observed.

Table 3. Getis–Ord results for hot spots and cold spots detected in the Caribbean and Pacific regions.

	Pacific		**Caribbean**	
Gi	**Number**	**%**	**Number**	**%**
Cold spot 99%	473	6.09%	393	9.55%
Cold spot 95%	358	4.61%	183	4.45%
Cold spot 90%	304	3.92%	159	3.86%
Not significant	5539	71.4%	2742	66.6%
Hot spot 90%	156	2.01%	77	1.87%
Hot spot 95%	267	3.44%	116	2.82%
Hot spot 99%	658	8.48%	441	10.7%
Total	7755	100%	4111	100%
Total hot + cold spot (99, 95, and 90%)	2216	28.5%	1369	33.3%
Total hot + cold spot (99%)		14.58%		20.28%

We take into account hot and cold spots with 99% significance, and this index allows for spatializing the significant points locally, and thus identifying the locations of cold spots (negative values—coastal erosion) and hot spots (positive values—sedimentation). On the Colombian Caribbean coast, cold spots were found in the Salamanca bar (Magdalena department); the northern area of the department of Atlántico, between the mouth of the Magdalena river (delta) and the low coasts to the southwest (beaches, littoral spikes); the area near the mouth of the Canal del Dique (delta) (department of Bolívar); sectors of fluvial and marine terraces in the department of Córdoba; and south of the mouth of the Turbo River in Antioquia and the beach sectors in the department of Chocó (Figure 7a). The hot spots, on the other hand, were located in the department of Bolívar, and correlated with some coastal rocky points and the deltas of the Canal del Dique, the Tinajones in Córdoba, and the Atrato in Antioquia (Figure 8a).

On the other hand, in the Colombian Pacific, due to its variability, fewer clustered areas and greater levels of dispersion (at 99%, 95%, and 90% significance) were observed. Regardless, cold spots were evident to the north of the department of Chocó, on the embedded beaches, and were more prevalent towards the south, that is, on the low coasts, which means that the sedimentation values in the mouths were higher. Another region of interest was in the delta of the Sanquianga river in Nariño. Hot spots were observed on the lower coasts of Valle del Cauca and in the interiors of bays, where mangrove swamps predominate. Nariño contains hot spots to the south of the Sanquianga sector, along almost the entire coastline, and these relate to the low coasts and the delta of the Mira River (Figure 8b).

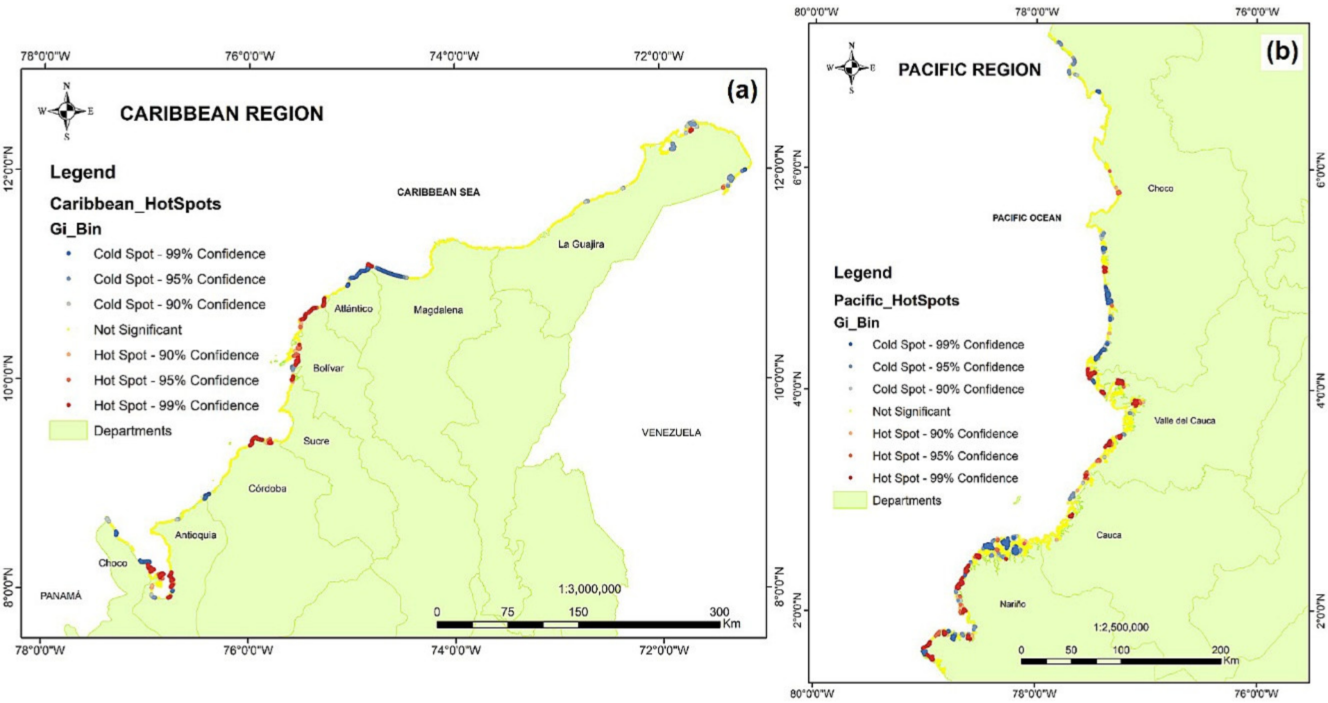

Figure 8. Locations of points with maximum negative values, indicating cold spots or sites undergoing coastal erosion (blue points) and sedimentation processes (red points), and those with high positive values indicating hot spots, for all coastal departments of the Caribbean (**a**) and the Colombian Pacific (**b**) coasts.

4.2.3. Local Moran's Index

The results of the I Moran local tests (Anselin) show significant local clustering patterns. The numbers of High–High and Low–Low cluster observations for the Pacific and Caribbean regions are presented in Table 4. High–High cluster (HH) observations represent points with positive values (sedimentation), which have z-scores indicating elevated BMI compared to the rest of the point, and are also surrounded by other points that have similarly high BMI z-scores (positive). The opposite is true for Low–Low (LL) groups (negative—erosion). In the Caribbean, there were 402 High–High and 491 Low–Low statistically significant spatial cluster observations, representing 9.7% and 11.9% of the sample, respectively. In the Pacific, there were 526 HH observations (6.7%) and 556 LL observations (7.1%).

Table 4. Total number of observations for the Local Moran's Index.

LISA	Pacific		Caribbean	
	Number Observations	**%**	**Number Observations**	**%**
HH	526	6.78%	402	9.78%
LL	556	7.17%	491	11.94%
LH	231	2.98%	40	0.97%
HL	177	2.28%	28	0.68%
Not significant	6265	80.79%	3150	76.62%
Total	7755	100%	4111	100%

Points with high or low neighborhoods of the Local Moran's Index are shown, with the High-High (coastal sedimentation) and Low–Low (coastal erosion) areas identified. In the Caribbean, isolated HH and LL points can be observed in the beach sectors corresponding to the center of the department of La Guajira, as well as to the interiors of the bays; LL points are also observed in the Salamanca bar (dep. Magdalena) and to the southwest of the mouth of the Magdalena River, interspersed with clusters of HH–LL–HH. In later periods, in the department of Bolívar, several separate clusters of HH predominate, where beaches, coastal lagoons, and the delta of the Canal del Dique are located; the delta of the river Sinú presents HH, similar to the delta of the river Atrato. Finally, an LL cluster was evident on the terraces of the departments of Córdoba and Antioquia, in addition to the beach areas of Chocó (Figure 8a). Visualizing the HH and LL clusters in the Pacific was more difficult, due to their dispersion into four clusters, but the groups were consistent on the shoreline from Cabo Corrientes in Chocó to the southern border with Ecuador (Figure 9b).

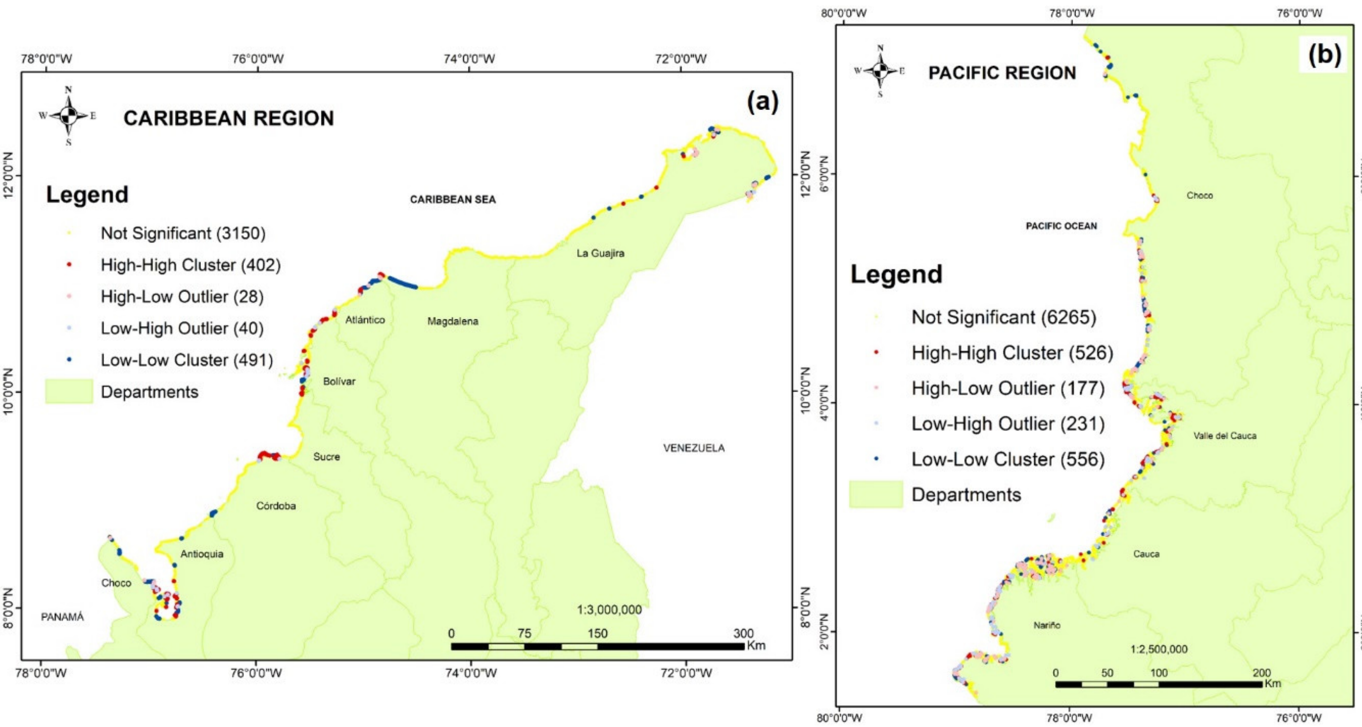

Figure 9. Spatial autocorrelation LISA cluster (Local Moran's I) of the phenomenon of coastal erosion in the Caribbean (**a**) and the Colombian Pacific (**b**). Hot spot = sedimentation (red); cold spot = erosion (blue). HH = Sh, LL = Ec, LH = Eo, HL = So.

On the other hand, Figure shows that the slope of the linear equation of the percentages of the I Local Moran groups is greater in the Caribbean than in the Pacific, with greater significance in the Caribbean and a greater dispersion in the Pacific.

In the Caribbean, localization correspondence with hot spots and cold spots is observed, while in the Pacific, we see dispersion between the four groups. In this region, the Getis–Ord index is more effectively visualized, despite maintaining dispersion values.

These results help to define the more statistically intense zones undergoing erosion and coastal sedimentation, through the values of neighborhoods, grouping and distance of the two processes as a whole.

4.2.4. Spatial Clustering by Coastal Erosion and Sedimentation

The global and local Moran's Index between the lagged values of the EPR and the EPR values show that in the Caribbean, there is greater clustering and a High–High and Low–Low cluster distribution (Figure 10a), while in the Pacific, there is less clustering and greater distribution between the four types (Figure 10b). Similarly, the above can also be observed and verified spatially through the LISA cluster, wherein, for the Colombian

Caribbean, areas such as the Salamanca bar show grouping based on Low–Low, and the delta Tinajones shows High–High cluster grouping.

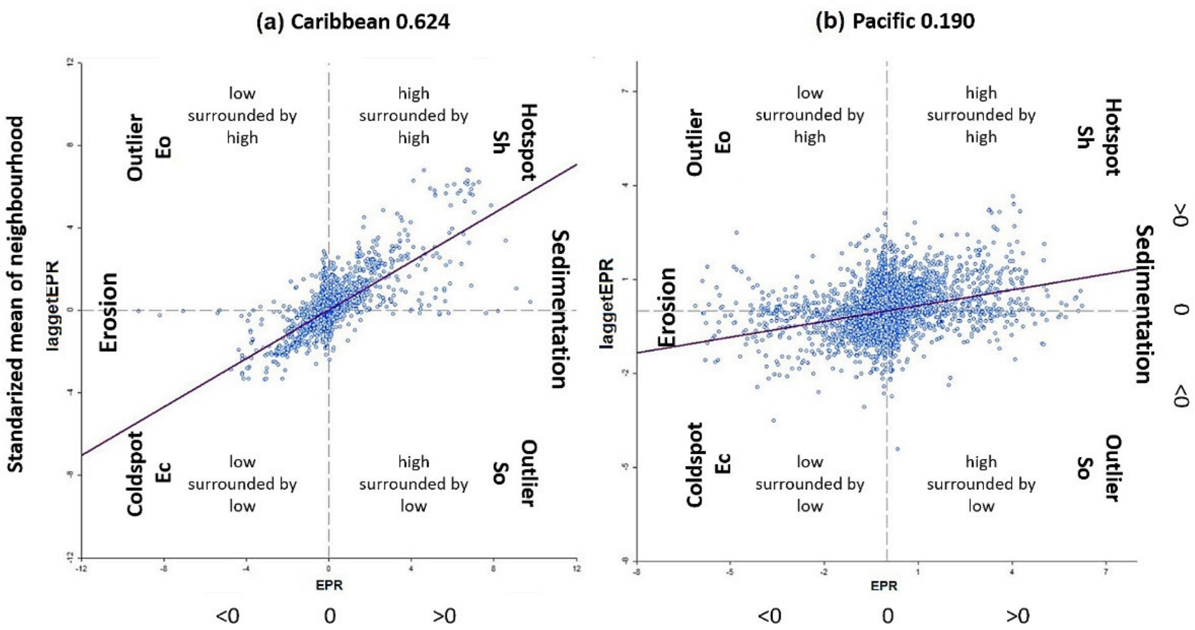

Figure 10. Graph of the spatial autocorrelation analysis (Global and Local Moran's Index) between lagged EPR values and EPR values of the coastal erosion phenomenon in the Caribbean (**a**) and the Colombian Pacific (**b**). Hot spot = sedimentation; cold spot = erosion. HH = Sh (sedimentation hot spot), LL = Ec (erosion cold spot), LH = Eo (erosion outlier), HL = So (sedimentation outlier). Adapted from Eamer and Walker, 2013; Nelson and Boots, 2008; Walker et al., 2013 [28,49,50].

One way of understanding Figure 10, which was adapted from Eamer and Walker, Nelson and Boots, and Walker et al. [28,49,50], is to relate the values of the Global and Local Moran's Indices with the erosion and coastal sedimentation processes of the Pacific and Caribbean regions, as follows: Caribbean—we observed greater sloping of the lagged EPR data, which means that the values of HH and LL (hot spot and cold spot) are separated from those of HL and LH (outlier), showing a Global Index of greater significance (0.624). However, we observe that the erosion (Ec) and sedimentation (Sh) processes are grouped together and are more intense, depending on the geoform upon which they are located. Pacific—there is less sloping in the lagged EPR data, which indicates that the values of HL and LH (outlier) are higher and are closer to those of HH and LL (hot spot and cold spot), with a low Global Index (0.190) and near randomness with low clustering. This verifies that the erosion (Ec) and sedimentation (Sh) processes show greater variability in space, close to the erosion outlier (Eo) and sedimentation outlier (So).

All this can be observed in the graphs of changes in the coastline (Figures 4–7), which show that in the Caribbean, there are localized and wide groups of erosion or sedimentation (depending on the geoform), while in the Pacific, there is intense variability between erosion and sedimentation.

The local Moran's Index and Getis–Ord index show similarities in the Caribbean, and it is possible to differentiate the significant points, but in the Pacific, it is not possible to observe the significant points using the Local Moran's I, as the dispersion and complexity of coastal areas influence this aspect (Figures 8 and 9). The percentages (indicators of each point) of the hot spot–cold spot and significant HH-LL points indicate that there are more significant locations in the Caribbean, and greater dispersion in the Pacific (Figure 11). The foregoing coincides with what is presented in Figure 10. Ultimately, the results are similar for the two local statistics.

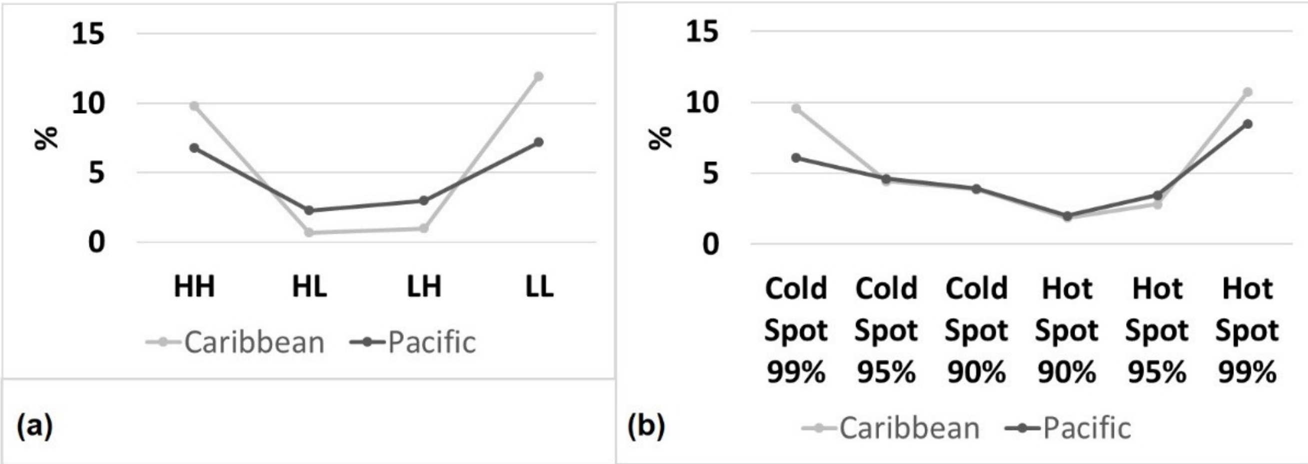

Figure 11. Comparison of the percentages between (**a**) Local Moran's Index and (**b**) Getis–Ord Index.

When observing the spatial results of the Local Moran's Index and the low and high coasts of Colombia, in the Caribbean and Pacific regions, the HH and LL groups generally coincide with low coasts (Figure 12). This corresponds to the real situation, since these coasts contain unconsolidated materials and have high variability, presenting high rates of coastal erosion and sedimentation, such as beaches, long beaches, pocket beaches, deltas, barrier islands, littoral bars, and mangrove swamps.

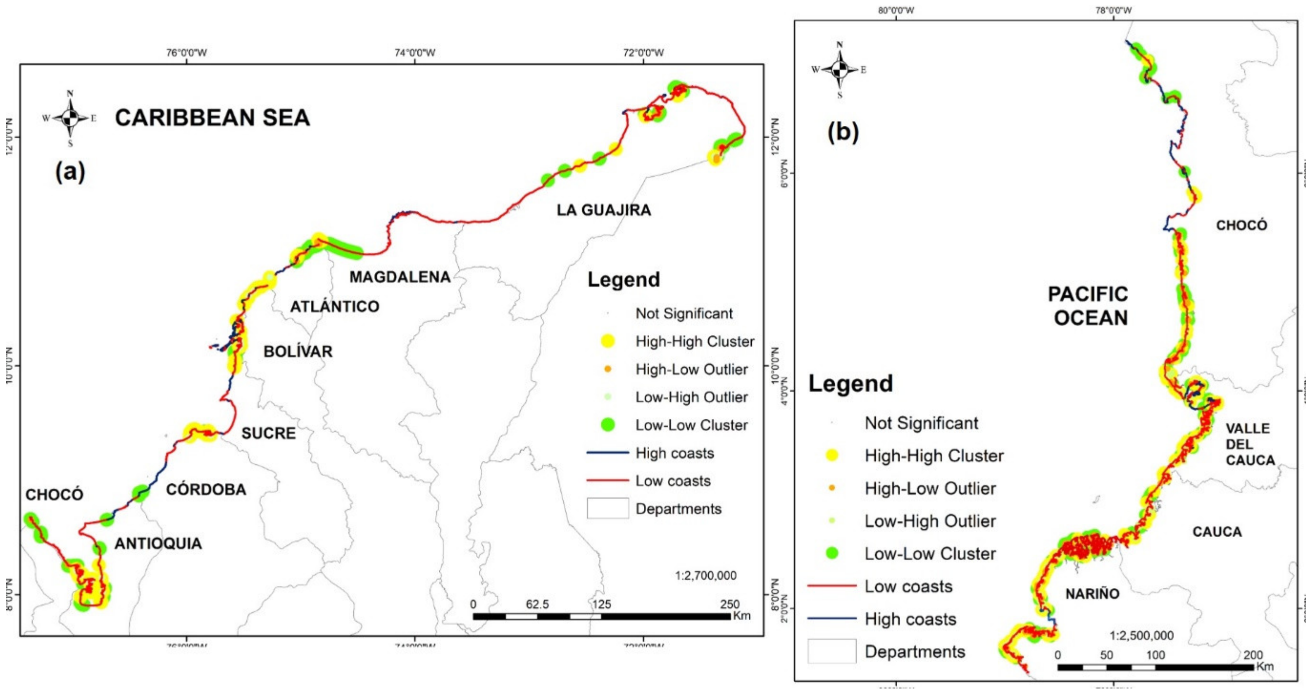

Figure 12. Comparison between the Local Moran's Index and the low coasts (sandy, muddy coasts, etc.) and high coasts (cliffs) for the Caribbean region (**a**) and the Pacific region (**b**).

As already mentioned, the locations of the significant points between the Local Moran's Index and the Getis–Ord Index (Figures 8, 9 and 12) coincide significantly. The results of the local indices as a whole, along with observations, were compared with the coastal physiographic units [80,81]. It was observed that the significant points manifest certain characteristics in relation these physiographic units; in the Caribbean, the *Peninsula de La Guajira* unit contains some significant points, but the next unit, the *Sierra Nevada de Santa Marta*, is characterized by cliffs, and does not present any significant point. Then, the unit

Delta of the Magdalena River, which encompasses the Ciénaga Grande de Santa Marta up to the mouth of the Canal del Dique, presents large groupings of points, both positive and negative. The *Sabanas del Caribe* unit corresponds to the department of Sucre; this unit had no points, while the unit *Valle of the Sinú and Alto San Jorge rivers* only contained a grouping in the delta of the Sinú River and some points on the cliffs of the terraces. Finally, the *Gulf of Urabá* unit contained several significant points, correlated with the mouths of the Atrato and Turbo rivers and the flood zones. The location of the significant points of the Colombian Caribbean coincides with the results of the study carried out by Rangel et al. [11], which shows the changes in the coastline until the year 2015, identifying from the observation of its results the critical points of coastal erosion. This confirms the benefits of using spatial analysis indices for coastal erosion and sedimentation processes.

In the Pacific, the *Serranía del Baudó* unit covers the entire north of the Choco department, from Cape Corrientes to the sector on the Caribbean coast, which behaves in the same way, with significant points on the beaches embedded between cliffs (both in the Pacific and in the Caribbean). The two remaining physiographic units of the Pacific are *the alluvial valleys of the Atrato and San Juan rivers* and *the Pacific coastal plains*. These two units are characterized by low alluvial coasts, and are where the largest number of dispersed and variable significant points was observed.

The significant points, which are obtained from the statistical spatial analysis, show which areas are where the greatest processes of coastal erosion and sedimentation are concentrated, matching with the analysis carried out in chapter 4.1 (*Variation in the Colombian coastline 1986–2016—regional characteristics of Caribbean and Pacific coasts-).* Therefore, the Local Moran and Getis–Ord indices are useful tools to statistically and spatially identify critical points of coastal erosion and sedimentation, supporting the interpretation made from the observation of the DSAS results.

5. Discussion

Coastal erosion (sedimentation) is a phenomenon that occurs in areas or extensions with similar conditions [82], but at longer temporal scales, regional patterns arise that are related to the configuration of the coast and geomorphological units, and their geographic extent depends on the homogeneity/heterogeneity of the coast. Each region shows variations in the level of clustering; that is, certain clustering patterns emerge. In this way, we can use the spatial autocorrelation law to determine the nature of the phenomenon for each zone or region, whether it works in a punctual or zonal way, and whether the conditions are different or similar.

The above-mentioned is important because of the future increase in shoreline projections on low-lying coasts, such as beaches, barrier islands, mudflats, etc., which should be treated with great care since the change trends on the coasts due to erosion and accretion are not uniform in time and space [34,83]. The record of shoreline change shows short-term variability, and change occurs in response to different cyclic factors [34,35], which vary from days to millennia in scale; for example, Galal and Takewaka [84] proposed patterns of shoreline response during a storm (short-term), and correlated these with wave energy, obtaining patterns of variability on a small scale. Furthermore, this was not a typical study of shoreline changes, but it has yielded regional patterns of these changes that can improve future projections of the shoreline, as proposed by Vousdoukas et al. [16], Crowell et al. [34], and Douglas and Crowell [35].

The results also indicate differences between the Caribbean region and the Colombian Pacific in terms of erosion and sedimentation phenomena in the coastal zone [2]. On the one hand, in the Caribbean, erosion and accretion processes occur in large areas or blocks, such as bars, coastal lagoons, deltas, etc. On the other hand, in the Pacific, large grouped areas showing erosion or accretion processes are not present, and high variability can be observed across the shoreline. Additionally, anthropic pressure is much higher in the Caribbean, which also influences the coastline via human impacts related to the destruction of certain geographical features, coastal geoforms, and geodiversity [4]. This alters the natural evolution of the coast and generates coastal erosion or sedimentation.

The data in Table 5 allow us to propose conceptual models of the regional patterns of coastal erosion and sedimentation, which are supported by Figure 13, for the Caribbean and Pacific regions. First, with more coastal geomorphological units (heterogeneity), a tendency may arise for greater clustering (represented by coastal erosion and sedimentation) (Figure 14a). Second, when the geomorphological units are larger (homogeneity), the level of clustering is smaller (Figure 14b).

Table 5. Values illustrating the relationship between Global Moran's Index, the geomorphological units, the number of repetitions of geomorphological units, and the sizes of geomorphological units.

Region	Moran's I	Geomorphology Units	Number of Repetitions	Size Units (Geomorphology Units/# Repetitions)
Caribbean	0.624	41	2511	61
Pacific	0.190	23	7755	337

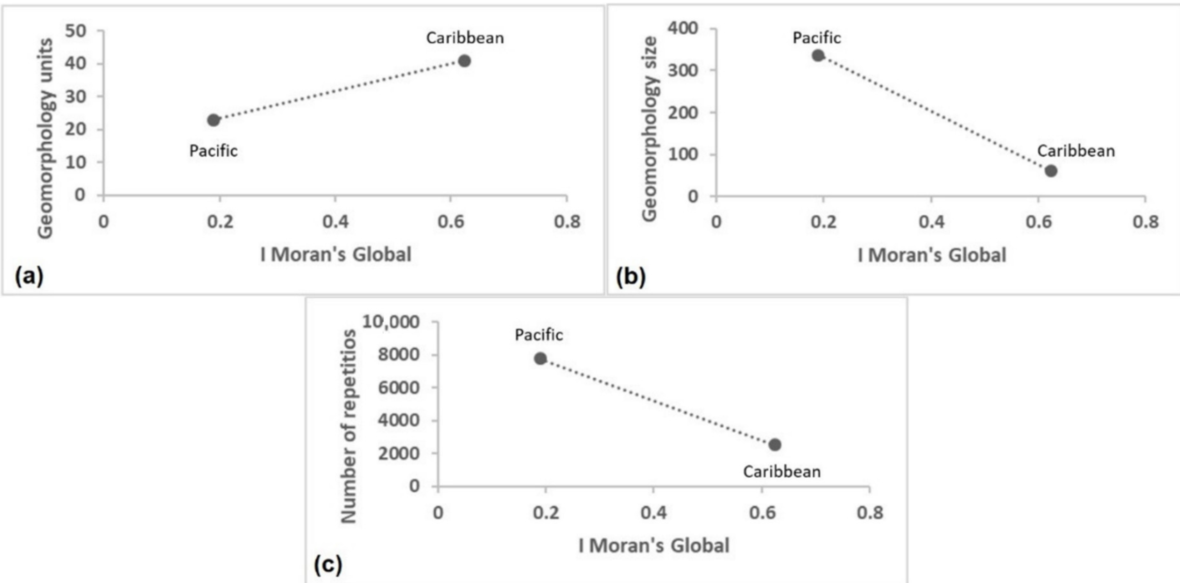

Figure 13. Values from Table 5 expressed graphically. This shows the relationship of the Global Moran's Index with the geomorphological units (**a**), the sizes of the geomorphological units (**b**), and the number of repetitions of the geomorphological units (coastal complexity) (**c**) of the Pacific and Caribbean regions.

Another relevant factor is the coastal complexity, represented by the number of repetitions of geomorphological units for each region (Figure 13c). A low level of clustering (Global Moran's Index), as is seen in the Pacific, is related to high coastal complexity, which is represented in the number of repetitions of the geomorphological units of each region; on the other hand, the high level of clustering in the Caribbean (Global Moran's Index) manifests low coastal complexity (Figure 14c). This is supported by the spatial distribution in the results of the Local Index (Figures 8 and 9) and by the lagged EPR points (Figure 10). This contradicts, or complements, the previous theory by relating the Global Index to the size and number of geomorphological units (Figure 14a,b).

Given the complexity of the coasts, it can be observed that HH and LL (Local Index) grouping occurs in areas with a specific geoform, taking into account the size (neighborhood and distance). In the Caribbean, this occurs in areas such as deltas and coastal bars or large terraces. There are no intercalations of smaller-scale geoforms, as is seen in the Pacific, which reduces the coastal complexity of the region. In the Pacific, as already mentioned, high coastal complexity is maintained due to the intercalation of smaller geoforms (estuaries' mouths, bars and beaches, and the sequence is repeated), unified within a few geomorphological units associated with mangrove swamps, estuaries, and barrier islands, which induces complexity in the configuration of the coast at a low scale as well as regional geomorphological homogeneity, due to the presence of fewer geomorphological units. All this is indicated by the low significance of the Global Index.

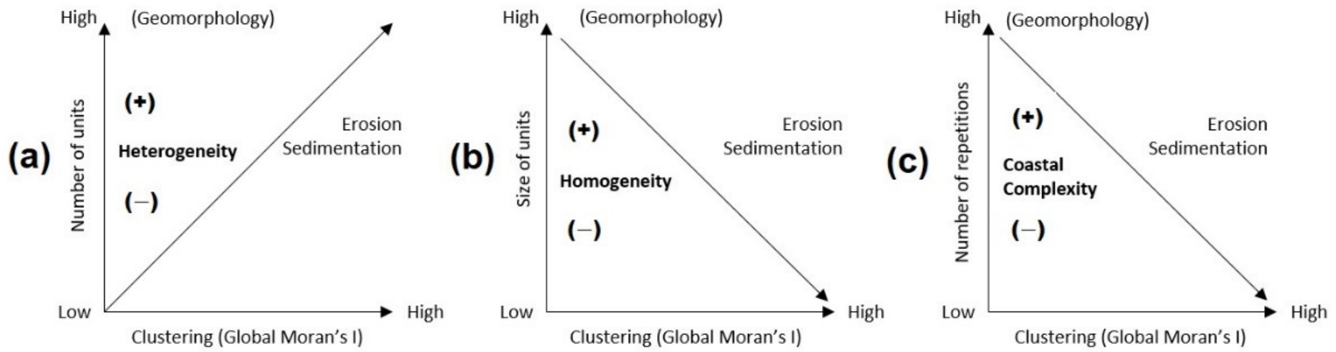

Figure 14. Conceptual diagram of the interaction between (**a**) geomorphology units (heterogeneity) and clustering (Global Moran's Index); (**b**) the sizes of geomorphology units (homogeneity) and clustering (Global Moran's Index); and (**c**) the number of repetitions of geomorphologic units (coastal complexity) and clustering (Global Moran's Index) to indicate regional patterns of coastal erosion and sedimentation.

Coastal erosion is a chronic phenomenon; it is not a one-time event [2]. It shows a high degree of variability in space and time, which depends on the conditions of the intrinsic nature of the phenomenon, as well as the physical, environmental, and anthropic conditions of each region [3]. Different studies around the world support the previous affirmations. In the Mediterranean, for example, the results of the coastline analyses of Awad and El-Sayed [85] showed alternation of erosion and coastal sedimentation over a time period of 34 years, and in addition, clustered by zones of homogeneous results (four zones of erosion and three of accretion). Finally, they consider that the triggering factors are human activities and waves as the main factor in coastal dynamics. Molina et al. [86] attribute the results of coastal erosion to local conditions and state that the erosion rate classifications should not be the same for each place. Borzi et al. [87] present three factors as the main modulators of coastal erosion and clustered under specific characteristics: deltas (rivers), the dune–beach relationship, and protection infrastructure. The results of Molina et al. [88] showed clustering in deltas, pocket beaches, and infrastructure zones.

Studies in the Pacific area also support our claims. Duan et al. [89], on the coasts of China, clustered their coastal erosion and sedimentation results into rocky, beachy, muddy, and anthropic coasts. Martinez et al. [90] carried out multi-temporal analyses for different beaches in Chile; their results are attributed to processes derived from local regional conditions, such as the different effects of seismic tectonics, e.g., tsunamis, the up-lift, and subsidence. Godwyn-Paulson et al. [91] analyzed the effects on the coastline produced by the sea swell event, where new local conditions, such as geomorphology and bathymetry, are the predominant factors in the results. Finally, Godwyn-Paulson et al. [92] mention that the migration pattern of the coast exhibits different behavior depending on the coastal environment in a particular region; for example, beaches are highly vulnerable compared to rocky coasts. This study relates triggering factors and landforms, and the results showed that the areas of greatest fluctuation are estuarine rivers and beaches. All the previous studies analyzed coastal erosion and sedimentation in space and time, under local conditions that allow clustering of the phenomenon, supporting our assertions. Despite the environmental differences in the world, such as areas with macro- or micro-tidal systems, the processes of coastal erosion and sedimentation present fluctuations that depend on local conditions, with different levels of clustering.

So, coastal erosion, being a chronic event, allows for its spatial behavior to be evaluated and, as such, we can define or conceptualize the phenomenon [41]. This study indicated that coastal erosion is a phenomenon with positive spatial autocorrelation; that is, it shows a certain degree of clustering, and its result is not random, nor does it happen in a dispersed way; it occurs in zones or areas that are most susceptible, which means that its occurrence depends on the presence of units with certain conditions, in which similar values are grouped. In this order of ideas, the Colombian Caribbean presents a higher degree of autocorrelation than the Pacific, which is generated by the differences in the environmental (geological and geomorphological, climatic, oceanographic, and anthropic) conditions of each region.

One of the main reasons why spatial autocorrelation is important is that it is derived from independent observation; that is, its concern is with evaluating the phenomenon and its intrinsic conditions [32]. If autocorrelation is present in coastal erosion (which starts with measuring the numbers of nearby objects compared to other nearby objects), this phenomenon will tend to present greater coherence between its nearby objects, and independent evaluation allows for it to be redefined, which is an advantage offered by the use of statistics to evaluate physical phenomena, such as this one.

Based on the concept of autocorrelation, under the concepts of coastal erosion and sedimentation, we can consider the loss or gain of territory in relation to the sea. However, we must also consider that these phenomena occur in areas or extensions of different sizes, under similar conditions, and that their level of impact will depend on the degree of clustering of the conditions. Together, this offers a comprehensive approach that considers the conditions and factors that influence coastal erosion and sedimentation. In addition, it illustrates how the configuration of the coastal zone influences regional patterns of coastal erosion. These results can be useful for planning purposes, because the greatest restrictions on land use would be imposed on shorelines having the highest erosion rates as proposed by Crowell et al. [34], and for the association with geomorphological units used to pay attention to other sectors of the coasts of the country with incipient erosion.

6. Conclusions

The clustering levels of coastal erosion and sedimentation of the Colombian Pacific and Caribbean are modulated by the different geomorphological characteristics of each of these regions. It was possible to define the high level of clustering in the Caribbean region, and the low level of clustering (or dispersion) in the Pacific. This means:

1. Caribbean: Significant areas here display low complexity, extensive spaces, and geomorphological unification (Local Index). This area has greater regional significance (Global Index). It has a greater slope of lagged EPR values.
2. Pacific: In areas with greater significance, larger sizes are attained. However, in terms of scale (Local Index), coastal complexity (mouth, islands, bars, beach, mouth, etc.) is indicated by larger geoforms (e.g., mangrove swamps), which generates significance in confined or ungrouped areas. This region has less significance (Global Index). The area is ungrouped and dispersed, with lower slopes of the EPR lagged-value curve, and HH and LL predominate, but HL and LH show more significant values here than in the Caribbean, which aids in differentiation.

It was possible to verify the efficiency of the spatial autocorrelation methods to characterize the processes of coastal erosion and sedimentation in the two coastal regions of the country. The Global Index method can be used for a general characterization of the two regions, since it allows defining the grouping level of each one, while the Local method (Moran and Getis) allows a visualization of significant data effectively and spatially. In addition, the Local Moran and Getis–Ord indices are useful tools to identify critical points of coastal erosion and sedimentation statistically and spatially, supporting or replacing the interpretation obtained from the observation of the DSAS results.

According to the results, three conceptual models can be proposed that relate the indices with the geomorphological characteristics: (1) the greater the geomorphological heterogeneity, the greater the grouping; (2) the greater the geomorphological homogeneity, the lower the degree of clustering; (3) the greater the geomorphological complexity, the lower the clustering.

Our findings support the proposal of a new reliable method to assess coastal erosion at a regional scale to support decision-making processes, through spatial autocorrelation analysis (Global Moran index, Local Moran index, and Getis–Moran index).

Author Contributions: Conceptualization, O.C. and C.R.-V.; methodology, O.C.; software, O.C.; validation, O.C and C.R.-V.; formal analysis, O.C.; investigation, O.C.; resources, C.R.-V.; writing—original draft preparation, O.C; writing—review and editing, O.C. and C.R.-V.; supervision, C.R.-V.; project administration, C.R.-V.; funding acquisition, C.R.-V. All authors have read and agreed to the published version of the manuscript.

Funding: This research received no external funding.

Institutional Review Board Statement: Not applicable.

Informed Consent Statement: Not applicable. The study did not involve humans or animals.

Data Availability Statement: Please contact the information systems laboratory LabSIS (INVEMAR): constanza.ricaurte@invemar.org.co.

Acknowledgments: This work was carried out by the project "Basic and applied research of renewable natural resources and the environment in the coastlines and marine and oceanic ecosystems of national interest", activity 2.1.6: Information on geohazards for risk management, that was provided by the National Investment Projects Bank (BPIN). The authors thank the researchers from the Marine and Coastal Geosciences—GEO (INVEMAR) program who provided support in this process. They thank the Information Systems Laboratory—LabSIS (INVEMAR) for its support in the downloading and georeferencing of images. We thank the reviewers for their comments and suggestions.

Conflicts of Interest: The authors declare no conflict of interest.

References

1. Bracs, M.A.; Turner, I.L.; Splinter, K.D.; Short, A.D.; Mortlock, T.R. Synchronised patterns of erosion and deposition observed at two beaches. *Mar. Geol.* **2016**, *380*, 196–204. [CrossRef]
2. Ricaurte-Villota, C.; Coca, O.; González, M.; Bejarano-Espinosa, M.; Morales, D.F.; Correa-Rojas, C.; Briceño-Zuluaga, F.; Legarda, G.; Arteaga, M. *Amenaza y Vulnerabilidad Por Erosión Costera en Colombia: Enfoque Regional Para La Gestión Del Riesgo*; Invemar: Santa Marta, Colombia, 2018; ISBN 9789588935423.
3. Coca, O.; Ricaurte-Villota, C. Validation of the hazard and vulnerability analysis of coastal erosion in the Caribbean and pacific coast of Colombia. *J. Mar. Sci. Eng.* **2019**, *7*, 260. [CrossRef]
4. Ferrer-Valero, N.; Hernández-Calvento, L.; Hernández-Cordero, A.I. Human impacts quantification on the coastal landforms of Gran Canaria Island (Canary Islands). *Geomorphology* **2017**, *286*, 58–67. [CrossRef]
5. *European Commission Living with Coastal Erosion in Europe: Sediment and Space for Sustainability*; Eurosion: Brussels, Belgium, 2004; ISBN 92-9167-186-X.
6. Posada, B.O.; Henao Pineda, W. *Diagnóstico de la Erosión En La Zona Costera del Caribe Colombiano*; Invemar: Santa Marta, Colombia, 2008; ISBN 9789589810491.
7. Posada, B.O.; Henao Pineda, W.; Guzmán Ospitia, G. *Diagnóstico de la Erosión Y Sedimentación En La Zona Costera del Pacífico Colombiano*; Invemar: Santa Marta, Colombia, 2009; ISBN 9789588448244.
8. Posada, B.O.; Henao Pineda, W.; Morales, D.F. *Diagnóstico de la Erosión Costera Del Territorio Insular Colombiano*; Invemar: Santa Marta, Colombia, 2011; ISBN 978-958-8448-44-2.
9. Cifuentes, M.A.; Rosero, L.V.; Selvaraj, J. Detección de cambios de la línea costera al norte del distrito de Buenaventura mediante el uso de sensores remotos. *Bol. Invest. Mar. Cost.* **2017**, *46*, 137–152. [CrossRef]
10. Coca, O.; Ricaurte-Villota, C. Análisis de la evolución litoral y respuesta de las comunidades afro-descendientes asentadas en la zona costera: Caso de estudio La Barra, Buenaventura, Pacífico Colombiano. *Entorno Geográfico* **2019**, 7–26. [CrossRef]
11. Rangel-Buitrago, N.G.; Anfuso, G.; Williams, A.T. Coastal erosion along the Caribbean coast of Colombia: Magnitudes, causes and management. *Ocean Coast. Manag.* **2015**, *114*, 129–144. [CrossRef]
12. Gutierrez-Valderrama, J.E.; Carvajal, A.F.; Pabón, J.D.; Ruiz, F.; Cusva Verdugo, A.; Nieto, V.; Lecanda, X.; Rodríguez, J.; Mendoza, J.; Álvarez, J.C.; et al. *Tercera comunicación nacional de Colombia*; Unidas, N., Ideam, P., Eds.; IDEAM: Bogotá, Colombia, 2017; p. 122.

13. Castelle, B.; Masselink, G.; Scott, T.; Stokes, C.; Konstantinou, A.; Marieu, V.; Bujan, S. Satellite-derived shoreline detection at a high-energy meso-macrotidal beach. *Geomorphology* **2021**, *383*, 107707. [CrossRef]
14. Luijendijk, A.; Hagenaars, G.; Ranasinghe, R.; Baart, F.; Donchyts, G.; Aarninkhof, S. The State of the World's Beaches. *Sci. Rep.* **2018**, *8*, 6641. [CrossRef]
15. Mentaschi, L.; Vousdoukas, M.I.; Pekel, J.F.; Voukouvalas, E.; Feyen, L. Global long-term observations of coastal erosion and accretion. *Sci. Rep.* **2018**, *8*, 12876. [CrossRef]
16. Vousdoukas, M.I.; Ranasinghe, R.; Mentaschi, L.; Plomaritis, T.A.; Athanasiou, P.; Luijendijk, A.; Feyen, L. Sandy coastlines under threat of erosion. *Nat. Clim. Chang.* **2020**, *10*, 260–263. [CrossRef]
17. Himmelstoss, E.A.; Henderson, R.E.; Kratzmann, M.G.; Farris, A.S. Digital Shoreline Analysis System (DSAS) Version 5.0 User Guide. *Open-File Rep.* **2018**, *1179*, 126.
18. Natesan, U.; Parthasarathy, A.; Vishnunath, R.; Kumar, G.E.J.; Ferrer, V.A. Monitoring Longterm Shoreline Changes along Tamil Nadu, India Using Geospatial Techniques. *Aquat. Procedia* **2015**, *4*, 325–332. [CrossRef]
19. Thieler, E.R.; Himmelstoss, E.A.; Zichichi, J.L.; Ergul, A. *The Digital Shoreline Analysis System (DSAS) Version 4.0—An ArcGIS Extension for Calculating Shoreline Change*; US Geological Survey: Reston, VA, USA, 2009; ISBN 2008-1278.
20. Coca, O.; Ricaurte-villota, C.; Morales, D.F. Modelo de gestión y análisis del riesgo por erosión costera. Caso de estudio departamento de Córdoba. In *Investigaciones en Gestión del Riesgo de desastres para Colombia. Avances, perspectivas y casos de estudio*; Comisión Nacional Asesora para la Investigación en Gestión del Riesgo de Desastres (CNAIGRD): Bogotá, Colombia, 2021; pp. 326–356. ISBN 9789585509191.
21. Kuleli, T.; Guneroglu, A.; Karsli, F.; Dihkan, M. Automatic detection of shoreline change on coastal Ramsar wetlands of Turkey. *Ocean Eng.* **2011**, *38*, 1141–1149. [CrossRef]
22. Radosavljevic, B.; Lantuit, H.; Pollard, W.; Overduin, P.; Couture, N.; Sachs, T.; Helm, V.; Fritz, M. Erosion and Flooding—Threats to Coastal Infrastructure in the Arctic: A Case Study from Herschel Island, Yukon Territory, Canada. *Estuaries and Coasts* **2016**, *39*, 900–915. [CrossRef]
23. Cliff, A.; Ord, K. The Problem of Spatial Autocorrelation. In *Studies in Regional Science*; Scott, A., Ed.; Pion: London, UK, 1969; pp. 25–55.
24. Goodchild, M.F. *Spatial autocorrelation*; Geo Books: Norwich, UK, 1986; ISBN 0860942236.
25. Tobler, W.R. A Computer Movie Simulating Urban Growth in the Detroit Region. *Econ. Geogr.* **1970**, *46*, 234–240. [CrossRef]
26. Pérez-Rubio, I.; Mende, A. Análisis espacial de susceptibilidad de erosión en una cuenca hidrográfica del trópico húmedo de Costa Rica. *Rev. Ciencias Ambient. (Trop. J. Environ. Sci.)* **2018**, *52*, 1–26. [CrossRef]
27. Javari, M. Spatial-temporal Variability of Seasonal Precipitation in Iran. *Open Atmos. Sci. J.* **2016**, *10*, 84–102. [CrossRef]
28. Nelson, T.A.; Boots, B. Detecting spatial hot spots in landscape ecology. *Ecography* **2008**, *31*, 556–566. [CrossRef]
29. Borrás Ramos, V. Análisis exploratorio de datos espaciales de pobreza: Aplicación 1996-2011 a tres ciudades de Uruguay (Montevideo, Maldonado y Salto). *Geogr. y Sist. Inf. Geográfica* **2019**, *11*. Sección I: 12–30.
30. Gordziejczuk, M.A.; Lucero, P.I. Turismo y calidad de vida: Un estudio de autocorrelación espacial aplicado a la ciudad de Mar del Plata, provincia de Buenos Aires, Argentina. *Cuad. Geogr. Rev. Colomb. Geogr.* **2019**, *28*, 23–42. [CrossRef]
31. Celemín, J.P. Autocorrelación espacial e indicadores locales de asociación espacial. Importancia, estructura y aplicación Spatial Autocorrelation and Local Indicators of Spatial Association: Importance, Structure and Application. *Rev. Univ. Geogr.* **2009**, *18*, 11–31.
32. Siabato, W.; Guzmán-Manrique, J. La autocorrelación espacial y el desarrollo de la geografía cuantitativa. *Cuad. Geogr. Rev. Colomb. Geogr.* **2019**, *28*, 1–22. [CrossRef]
33. Vilalta, C.J. Cómo enseñar autocorrelación espacial. *Econ. Soc. Territ.* **2005**. [CrossRef]
34. Crowell, M.; Leatherman, S.P.; Buckley, M.K. Shoreline Change Rate Analysis: Long Term Versus Short Term Data. *Shore Beach* **1993**, *61*, 13–20.
35. Douglas, B.C.; Crowell, M. Long-term shoreline position prediction and error propagation. *J. Coast. Res.* **2000**, *16*, 145–152.
36. Moore, L.J. Shoreline mapping techniques. *J. Coast. Res.* **2000**, *16*, 111–124.
37. Thieler, E.R.; Danforth, W.W. Historical shoreline mapping (I): Improving techniques and reducing positioning errors. *J. Coast. Res.* **1994**, *10*, 549–563.
38. Crowell, M.; Leatherman, S.P.; Buckley, M.K. Historical shoreline change: Error analysis and mapping accuracy. *J. Coast. Res.* **1991**, *7*, 839–852.
39. Ojeda Zújar, J.; Díaz Cuevas, M.D.P.; Prieto Campos, A.; Álvarez Francoso, J.I. Línea de costa y sistemas de información geográfica: Modelo de datos para la caracterización y cálculo de indicadores en la costa andaluza. *Investig. Geográficas* **2013**, 37–52. [CrossRef]
40. Genz, A.S.; Fletcher, C.H.; Dunn, R.A.; Frazer, L.N.; Rooney, J.J. The predictive accuracy of shoreline change rate methods and alongshore beach variation on Maui, Hawaii. *J. Coast. Res.* **2007**, *23*, 87–105. [CrossRef]
41. Hughey, S.M.; Kaczynski, A.T.; Porter, D.E.; Hibbert, J.; Turner-McGrievy, G.; Liu, J. Spatial clustering patterns of child weight status in a southeastern US county. *Appl. Geogr.* **2018**, *99*, 12–21. [CrossRef]
42. Romine, B.M.; Fletcher, C.H.; Frazer, L.N.; Genz, A.S.; Barbee, M.M.; Lim, S.C. Historical shoreline change, southeast oahu, Hawaii; Applying polynomial models to calculate shoreline change rates. *J. Coast. Res.* **2009**, *25*, 1236–1253. [CrossRef]
43. Ranasinghe, R. Assessing climate change impacts on open sandy coasts: A review. *Earth-Science Rev.* **2016**, *160*, 320–332. [CrossRef]

44. Bayram, B.; Acar, U.; Seker, D.; Ari, A. A novel algorithm for coastline fitting through a case study over the bosphorus. *J. Coast. Res.* **2008**, *24*, 983–991. [CrossRef]
45. García-Rubio, G.; Huntley, D.; Russell, P. Evaluating shoreline identification using optical satellite images. *Mar. Geol.* **2015**, *359*, 96–105. [CrossRef]
46. Liu, Q.; Trinder, J.; Turner, I.L. Automatic super-resolution shoreline change monitoring using Landsat archival data: A case study at Narrabeen–Collaroy Beach, Australia. *J. Appl. Remote Sens.* **2017**, *11*, 016036. [CrossRef]
47. Pardo-Pascual, J.E.; Almonacid-Caballer, J.; Ruiz, L.A.; Palomar-Vázquez, J. Automatic extraction of shorelines from Landsat TM and ETM+ multi-temporal images with subpixel precision. *Remote Sens. Environ.* **2012**, *123*, 1–11. [CrossRef]
48. Hagenaars, G.; de Vries, S.; Luijendijk, A.P.; de Boer, W.P.; Reniers, A.J.H.M. On the accuracy of automated shoreline detection derived from satellite imagery: A case study of the sand motor mega-scale nourishment. *Coast. Eng.* **2018**, *133*, 113–125. [CrossRef]
49. Eamer, J.B.R.; Walker, I.J. Quantifying spatial and temporal trends in beach-dune volumetric changes using spatial statistics. *Geomorphology* **2013**, *191*, 94–108. [CrossRef]
50. Walker, I.J.; Eamer, J.B.R.; Darke, I.B. Assessing significant geomorphic changes and effectiveness of dynamic restoration in a coastal dune ecosystem. *Geomorphology* **2013**, *199*, 192–204. [CrossRef]
51. Flint, C.; Harrower, M.; Edsall, R. But How Does Place Matter? Using Bayesian Networks to Explore a Structural Definition of Place. In *Proceedings of the The New Methodologies for the Social Sciences Conference*; University of Colorado: Boulder, CO, USA, 2000.
52. LeSage, J. *Spatial Econometrics Toolbox*; Universidad de Toledo: Toledo, Spain, 1999.
53. O'Loughlin, J.; Anselin, L. Geography of International Conflict and Cooperation: Theory and Methods. In *The New Geopolitics*; Don Ward, M., Ed.; Routledge: Philadelphia, PA, USA, 1992; pp. 11–38. ISBN 9781315075242.
54. Buzai, G.D. *Mapas Sociales*; Lugar Editorial: Luján, Argentina, 2007; ISBN 9789508924513.
55. Burt, J.; Barber, G.; Rigby, D. *Elementary Statistics for Geographers*; The Guilford Press: New York, NY, USA, 2009.
56. Laraia, B.A.; Blanchard, S.D.; Karter, A.J.; Jones-Smith, J.C.; Warton, M.; Kersten, E.; Jerrett, M.; Moffet, H.H.; Adler, N.; Schillinger, D.; et al. Spatial pattern of body mass index among adults in the diabetes study of Northern California (DISTANCE). *Int. J. Health Geogr.* **2014**, *13*, 48. [CrossRef]
57. Auchincloss, A.H.; Gebreab, S.Y.; Mair, C.; Diez Roux, A.V. A review of spatial methods in epidemiology, 2000-2010. *Annu. Rev. Public Health* **2012**, *33*, 107–122. [CrossRef]
58. Anselin, L. Local Indicators of Spatial Association—LISA. *Geogr. Anal.* **1995**, *27*, 93–115. [CrossRef]
59. Getis, A.; Ord, J.K. The Analysis of Spatial Association by Use of Distance Statistics. *Geogr. Anal.* **1992**, *24*, 189–206. [CrossRef]
60. Keith Ord, J.; Getis, A. Testing for local spatial autocorrelation in the presence of global autocorrelation. *J. Reg. Sci.* **2001**, *41*, 411–432. [CrossRef]
61. Ord, J.K.; Getis, A. Local Spatial Autocorrelation Statistics: Distributional Issues and an Application. *Geogr. Anal.* **1995**, *27*, 286–306. [CrossRef]
62. Anselin, L. Exploring Spatial Data with GeoDa: A Workbook. *Geography* **2005**, 244.
63. Moran, P.A.P. The spectral theory of discrete stochastic processes. *Biometrika* **1949**, *36*, 63–70. [CrossRef]
64. Moran, P.A.P. Notes on continuous stochastic phenomena. *Biometrika* **1950**, *37*, 17–23. [CrossRef]
65. Martínez, J.O.; González, J.L. *Evolución Histórica De Las Islas Barrera Del Sector de Buenaventura y El Naya*; Invemar: Santa Marta, Colombia, 1997; ISBN 9589595049.
66. Restrepo-López, J.C.; Ortíz -Royero, J.C.; Otero-Díaz, L.; Ospino-Ortiz, S.R. Transporte de sedimentos en suspensión en los principales ríos del Caribe colombiano: Magnitud, tendencias y variabilidad. *Rev. la Acad. Colomb. Ciencias Exactas, Físicas y Nat.* **2015**, *39*, 527. [CrossRef]
67. Restrepo, J.D.; López, S.A. Morphodynamics of the Pacific and Caribbean deltas of Colombia, South America. *J. South Am. Earth Sci.* **2008**, *25*, 1–21. [CrossRef]
68. Bernal, G.; Betancur, J. Sedimentología de Lagunas Costeras: Ciénaga Grande de Santa Marta y Ciénaga de Pajarales. *Boletín Investig. Mar. Costeras1* **1996**, 49–76. [CrossRef]
69. Restrepo, J.C.; Orejarena-Rondón, A.; Consuegra, C.; Pérez, J.; Llinas, H.; Otero, L.; Álvarez, O. Siltation on a highly regulated estuarine system: The Magdalena River mouth case (Northwestern South America). *Estuar. Coast. Shelf Sci.* **2020**, *245*, 107020. [CrossRef]
70. Fuentes Delgado, J.E. Desaparición de las islas: Cambios ambientales en el delta del río Magdalena desde la cartografía histórica. *Hist. y Espac.* **2022**, *18*, 159–192. [CrossRef]
71. Bastidas-Salamanca, M.; Ricaute-Villota, C. *Regionalización Oceanográfica, Una Visión Dinámica Del Caribe*; Invemar: Santa Marta, Colombia, 2017; ISBN 9789588935249.
72. Otero, L.J.; Ortiz-Royero, J.C.; Ruiz-Merchan, J.K.; Higgins, A.E.; Henriquez, S.A. Storms or cold fronts: What is really responsible for the extreme waves regime in the Colombian Caribbean coastal region? *Nat. Hazards Earth Syst. Sci.* **2016**, *16*, 391–401. [CrossRef]
73. Correa, I.; Morton, R. *Pacific Coast of Colombia BT—Encyclopedia of the World's Coastal Landforms*; Bird, E.C.F., Ed.; Springer: Dordrecht, The Netherlands, 2010; pp. 193–198. ISBN 978-1-4020-8639-7.
74. Martínez-Ardila, N.J. Amenazas naturales en el litoral Pacífico colombiano asociadas al ascenso del nivel del mar. *Cuad. Geogr. Rev. Colomb. Geogr.* **2005**, 83–96.

75. Castelle, B.; Guillot, B.; Marieu, V.; Chaumillon, E.; Hanquiez, V.; Bujan, S.; Poppeschi, C. Spatial and temporal patterns of shoreline change of a 280-km high-energy disrupted sandy coast from 1950 to 2014: SW France. *Estuar. Coast. Shelf Sci.* **2018**, *200*, 212–223. [CrossRef]
76. Wang, X.-Z.; Zhang, H.-G.; Fu, B.; Shi, A. Analysis on the coastline change and erosion-accretion evolution of the Pearl River Estuary, China, based on remote-sensing images and nautical charts. *J. Appl. Remote Sens.* **2013**, *7*, 073519. [CrossRef]
77. Currin, C.; Davis, J.; Baron, L.C.; Malhotra, A.; Fonseca, M. Shoreline change in the New River Estuary, North Carolina: Rates and consequences. *J. Coast. Res.* **2015**, *31*, 1069–1077. [CrossRef]
78. Cowart, L.; Walsh, J.P.; Corbett, D.R. Analyzing Estuarine Shoreline Change: A Case Study of Cedar Island, North Carolina. *J. Coast. Res.* **2010**, *265*, 817–830. [CrossRef]
79. Restrepo, J.D.; Kjerfve, B.; Correa, I.D.; González, J. Morphodynamics of a high discharge tropical delta, San Juan River, Pacific coast of Colombia. *Mar. Geol.* **2002**, *192*, 355–381. [CrossRef]
80. Karin, P.; Álvarez, S. Clasificación fisiográfica del terreno a partir de la inclusión de nuevos elementos conceptuales. *Perspect. Geográfica* **2009**, *1*, 181–218. [CrossRef]
81. Villota, H. Nuevos elementos conceptuales para la clasificación fisiográfica del terreno. *Rev. CIAF -St. Fe Bogotá* **1997**, *15*, 83–117.
82. Masselink, G.; Russell, P.; Rennie, A.; Brooks, S.; Spencer, T. The impacts of climate change on coastal geomorphology and coastal erosion relevant to the coastal and marine environment around the UK. *Mar. Clim. Chang. Impacts Partnersh. Sci. Rev.* **2020**, *2020*, 456–481. [CrossRef]
83. Galgano, F.A., Jr. Shoreline behavior along the Atlantic coast of Delaware. *Middle States Geogr.* **2008**, *41*, 74–81.
84. Galal, E.M.; Takewaka, S. The influence of alongshore and cross-shore wave energy flux on large- and small-scale coastal erosion patterns. *Earth Surf. Process. Landforms* **2011**, *36*, 953–966. [CrossRef]
85. Awad, M.; El-Sayed, H.M. The analysis of shoreline change dynamics and future predictions using automated spatial techniques: Case of El-Omayed on the Mediterranean coast of Egypt. *Ocean Coast. Manag.* **2021**, *205*, 105568. [CrossRef]
86. Molina, R.; Manno, G.; Re, C.L.; Anfuso, G.; Ciraolo, G. A methodological approach to determine sound response modalities to coastal erosion processes in mediterranean Andalusia (Spain). *J. Mar. Sci. Eng.* **2020**, *8*, 154. [CrossRef]
87. Borzì, L.; Anfuso, G.; Manno, G.; Distefano, S.; Urso, S.; Chiarella, D.; Di Stefano, A. Shoreline Evolution and Environmental Changes at the NW Area. *Land* **2021**, *10*, 1034. [CrossRef]
88. Molina, R.; Anfuso, G.; Manno, G.; Prieto, F.J.G. The Mediterranean coast of Andalusia (Spain): Medium-term evolution and impacts of coastal structures. *Sustainability* **2019**, *11*, 3539. [CrossRef]
89. Duan, P.; Li, J.; Wang, M.; Wu, J. Spatial-Temporal Analysis of the Coastline Changes in Fujian Province, China from 1995 to 2015. *J. Environ. Sci. Manag.* **2021**, *24*, 1–9. [CrossRef]
90. Martínez, C.; Grez, P.W.; Martín, R.A.; Acuña, C.E.; Torres, I.; Contreras-López, M. Coastal erosion in sandy beaches along a tectonically active coast: The Chile study case. *Prog. Phys. Geogr.* **2022**, *46*, 250–271. [CrossRef]
91. Godwyn-Paulson, P.; Jonathan, M.P.; Hernandez, F.R.; Muthusankar, G.; Lakshumanan, C. Coastline variability of several Latin American cities alongside Pacific Ocean due to the unusual "Sea Swell" events of 2015. *Environ. Monit. Assess.* **2020**, *192*, 1–12. [CrossRef]
92. Godwyn-Paulson, P.; Jonathan, M.P.; Roy, P.D.; Rodríguez-Espinosa, P.F.; Muthusankar, G.; Muñoz-Sevilla, N.P.; Lakshumanan, C. Evolution of southern Mexican Pacific coastline: Responses to meteo-oceanographic and physiographic conditions. *Reg. Stud. Mar. Sci.* **2021**, *47*, 101914. [CrossRef]